An Analysis of Alouette I

Plasma Resonance Observations

By

Robert F. Benson
NASA-Goddard Space Flight Center
Greenbelt, Maryland

April 1968

Presented at the NATO Advanced Study Institute on Plasma Waves in Space and in the Laboratory, Røros, Norway, April, 1968.

Abstract

The plasma resonances observed by the Alouette I satellite were analyzed to determine (a) whether the frequencies of the cyclotron harmonic resonances follow the harmonic relation $f_n = nf_H$, (b) the size of the resonant excitation region, and (c) the physical nature of the observed phenomena. The major observations were: (1) When high order cyclotron harmonic resonances were observed the frequencies of these resonances deviate from the above harmonic relation in that they correspond to lower values for f_H than do the lower order harmonics. (2) Some of the cyclotron harmonic resonant frequencies were found to be sensitive to changes in the electron density N, the maximum observed variation being $0.4 \pm 0.2\%$ for the $n = 3$ resonance when the value of the upper-hybrid frequency crosses the value of $3f_H$. (3) The frequency of occurrence of the nf_H resonances with $n > 4$ was highest when the velocity of the satellite $\vec{V}_s$ was approximately parallel to $\vec{B}$. (4) The duration of most of the plasma resonances depends on the angle β between $\vec{V}_s$ and $\vec{B}$; it increases with increasing $\cos \beta$ for the resonances at f_N (electron plasma frequency) and at nf_H when $n > 2$, but decreases for the resonance at f_T (upper-hybrid frequency). (5) Large periodic amplitude fluctuations of the order of 2-3 kc/sec were often observed during the decay of the f_T resonance in the high-latitude data (but never in the low-latitude data) and during the decay of the f_N resonance in the low-latitude data (but never in the high-latitude data). (6) Resonances of long duration were observed at f_N, f_T, and the lower harmonics of f_H when the radiating antenna (long antenna in this case) was far removed from a parallel configuration with $\vec{B}$. The major conclusions inferred from this analysis are: (1) The plasma resonance

at $3f_H$ is not well described by the often-applied electrostatic approximation to the dispersion equation, and it appears that the full electromagnetic equations must be retained in this case. The choice of the data regions precludes similar statements concerning the other resonances. (2) Some of the resonances of long duration can be interpreted as plasma waves with group velocities matched to the satellite velocity, and in some cases a preferred direction of propagation is indicated. The group velocity is predominately perpendicular to $\vec{B}$ for the f_T resonance and predominately parallel to $\vec{B}$ for the f_N and $3f_H$ resonances. The resonances of short duration (at the higher harmonics of f_H) are attributed to plasma waves of nearly zero group velocity. (3) The region of resonant excitation extends beyond the antenna sheath region but not beyond several antenna lengths from the satellite. (4) The natural spectral width of the nf_H resonances is less than 10 kc/s.

Introduction

Plasma resonances have been the subject of considerable interest in the fields of plasma physics and geophysics in recent years. In the field of plasma physics most of the research has been related to electron and ion cyclotron harmonic radiation observed in thermonuclear fusion oriented experiments. Other research has been initiated in an attempt to explain the Alouette I observations of a series of resonances excited by a transmitting antenna immersed in a plasma (Crawford, 1965; Crawford et al., 1967). In the field of geophysics a great deal of interest in plasma resonances centers around their potential use in electron density and magnetic field measurements from space vehicles since $f_N \propto N^{\frac{1}{2}}$ and $f_H \propto B$ where f_N is the electron plasma frequency, N is the electron density, f_H is the electron cyclotron frequency, and B is the total intensity of the magnetic field.

The plasma resonances observed by the Canadian satellite Alouette I are a by-product since the main purpose of the satellite was to obtain electron density profiles of the topside ionosphere. The satellite's sweep frequency sounder covers a range of 0.5 to 11.5 Mc/s every 18 seconds, and the resulting data can be analyzed directly in the amplitude vs. time format or can be converted to the conventional ionogram format (Fitzenreiter and Blumle, 1964); both formats are illustrated in Fig. 1. These resonances were first observed by Lockwood (1963); their identification and explanation were extended by Calvert and Goe (1963) who were the first to interpret them as plasma resonances. They are commonly observed at the frequencies f_N, f_H, harmonics of f_H, f_T, and its second harmonic $2f_T$ (see Table 1 for an explanation of the notation commonly used in this paper).

The cold plasma theory of electromagnetic wave propagation (Appleton-Hartree theory) predicts unique effects for the propagation modes at the frequencies f_Z, f_X, and f_N when the wave number $k = \frac{2\pi}{\lambda} \rightarrow 0$ and f_H and f_T when $k \rightarrow \infty$ (Bekefi, Chap. 7, 1966). In all of these cases the group velocity approaches zero, i.e., $\frac{\partial \omega}{\partial k} \rightarrow 0$. Sturrock (1961) considers this condition to be a suitable definition for a resonant situation since no energy is then lost by propagation. Similar resonant conditions are not predicted for the frequencies nf_H, $n = 2, 3, ---$ in cold plasma theory. The first attempt to explain the existence of resonances at these frequencies on the Alouette I data were based on the non-collective effects of the bunching of electrons (Lockwood, 1963; Johnston and Nuttall, 1964). Later work has centered on the collective behavior of the plasma, and has attempted to explain the observed long duration associated with the resonances in terms of solutions of the wave dispersion equation in warm plasma theory. Two different dispersion theory approaches have been considered - the first considers strictly electrostatic (longitudinal) oscillations of the plasma (Fejer and Calvert, 1964; Sturrock, 1965), whereas the second allows for transverse oscillations by considering the full electromagnetic equations (Shkarofsky, 1966; Shkarofsky and Johnston, 1965). For a discussion of the dispersion relations, see Bekefi (Chap. 1, 1966) and Stix (1962).

Fejer and Calvert (1964) stressed the requirement of low Landau damping in their attempt to explain the resonances of long duration observed by Alouette I. They simplified the dispersion relation for the electrostatic approximation by considering the region of small k and found solutions corresponding to the observed resonant frequencies when $\theta = 0$ and $\theta = \pi/2$,

where θ is the angle between $\vec{k}$ and $\vec{B}$. The solutions obtained were the following: $f = f_H$ and $f = f_N$ when $\vec{k}$ is approximately parallel to $\vec{B}$, and $f = f_T$ and $f = nf_H$ with $n = 2, 3, ----$ when $\vec{k}$ is approximately perpendicular to $\vec{B}$. The durations of the resonances were investigated by considering the spreading of a wave packet with low group velocity. The results indicated that when $0 < \theta < \pi/2$ the group velocity $\vec{V}_g$ is approximately perpendicular to $\vec{k}$ and the oscillations quickly die out, but when $\theta = 0$ or $\theta = \pi/2$ the direction of $\vec{V}_g$ is parallel to $\vec{k}$ and the oscillations are long lasting. Sturrock (1965) considered solutions of the electrostatic dispersion equation when $V_g = 0$ and used the infinitesimal dipole approximation to calculate the time dependence of the observed resonances. The calculated duration times greatly exceeded the observed durations; the discrepancy was attributed to the motion of the satellite out of the region of excitation. Deering and Fejer (1965) extended this approach by calculating both the space and time dependence of the field associated with the resonances.

Shkarofsky and Johnston (1965)(see also Shkarofsky, 1966) criticized the above work because the electrostatic approximation to the dispersion equation is used in the domain of small k. They also stressed the concept of matching the wave group velocity with the satellite velocity, rather than considering conditions of zero group velocity, and found that matching conditions could be satisfied for the nf_H resonances for all n when the waves were non-longitudinal but only for $n \leq 3$ when the waves were longitudinal. The calculated time durations associated with the electrostatic matching points were far greater than the observed durations whereas the calculations based on the electromagnetic matching points gave order-of-magnitude agreement. They infer that when both matching points are

possible, for a given resonance, the short wavelength electrostatic waves are more difficult to excite and are more strongly affected by antenna sheaths than the non-longitudinal waves. Their calculations indicate an excitation mechanism favoring the lower harmonics but a resonant relaxation after excitation favoring the higher harmonics. The frequency deviation $(f_n - nf_H)/f_n$ was found to be relativistically small for the non-longitudinal waves (this required the use of relativistic theory) but of a larger, and possibly detectable, magnitude for the longitudinal waves. A similar - but not as extensive - theoretical treatment has been given by Dougherty and Monaghan (1965).

This paper presents the results of an analysis of the Alouette I plasma resonances which was conducted to obtain information on the physical nature of the observed phenomena and to answer the following two questions:
(1) What is the interaction volume associated with the observed resonances?
(2) How close do the observed cyclotron harmonic resonant frequencies f_n agree with the harmonic law $f_n = nf_H$?

The first question is of importance in the measurement of electron density which is different in the sheath region surrounding the satellite than in the undisturbed medium. Both questions must be considered in the design of a magnetometer based on the observed cyclotron harmonic resonances since harmonic-recognition offers a possible method of distinguishing these resonances from the other plasma resonances, and the interaction volume determines the effect that a residual spacecraft field will have on the observations. Such a magnetometer could offer a method of measuring the earth's magnetic field from satellites without employing the long booms that are currently used to separate the magnetometer sensing element from

the main spacecraft. This may be of particular value in future satellites requiring several pairs of long antennas for electric field experiments similar to those proposed by Aggson et al., (1967).

The main problem in the investigation of the Alouette cyclotron harmonic resonances is that the exact value of the earth's magnetic field $\vec{B}$ is not known at the position of the satellite. The harmonic nature of the resonances can be investigated, however, if a reference field can be obtained that will provide accurate relative values from one resonance to another. Barrington and Herzberg (1966) investigated specially selected Alouette I ionograms containing reasonably long series of cyclotron harmonic resonances that were observed over a wide range of conditions. They calculated f_H for each resonance on a given ionogram from the relation $f_H=f_n/n$ and then used the mean of these values for the reference level on that ionogram. No deviations from a harmonic relationship were detected within their experimental accuracy of 1%.

The present analysis of Alouette I data attains an experimental accuracy of 0.2% or better by averaging the data from many ionograms. The problem of obtaining a reliable reference field was solved by imposing three restrictions on the selection of the data. First, only data from small spatial regions were considered. This restriction was necessary because existing model field calculations do not describe the earth's main field with the same precision over the entire earth (Cain, 1966). In small regions, however, the calculated field can be used to provide the reliable relative reference field values from one measurement to the next. In order to obtain a true data sample from each region, no attempt was made to select ionograms on the basis of the nature or number of resonances present since

such a selection would further restrict the data into a sub-class that is dependent on the orientation of the satellite's radiating antenna with respect to $\vec{B}$ (Lockwood, 1965). Second, only data collected over a time interval of approximately one year (mainly during 1963) were considered because the uncertainties associated with model field predictions of the geomagnetic secular variation (Cain and Hendricks, 1967) may be significant in the present analysis over longer intervals. Third, only data from magnetically quiet days were considered in order to safely ignore the effect of magnetic disturbance fields. These restrictions greatly reduce the amount of available data, but this limitation is more than compensated for by the resulting reference field (which provides accurate relative values of $\vec{B}$ as well as nearly constant value of $\vec{B}$) which can be used with confidence to investigate the Alouette I cyclotron harmonic resonances in a manner that can be described as a somewhat controlled plasma physics experiment in space.

Observations

Selection of data. The nearly circular polar orbit of Alouette I made it feasible to observe many satellite passes through a chosen region of interest. Five small regions were selected for the present analysis; the geographic coordinates, dipole latitude, and magnetic inclination corresponding to these regions are given in Table 2 together with the appropriate telemetry receiving stations. (The identification of the data in the figures is by station code rather than by region number.)

The criteria used for selecting the regions were the following: the availability of data, the frequency response of the Alouette I sounder, and the orientation of the earth's magnetic field vector with respect to the satellite's velocity vector. Region 1 was selected for a pilot study because the data from this region were readily available and the results could be compared with existing rocket measurements over Wallops Island, Virginia of the earth's magnetic field. Regions 2 and 3 were selected because they are located near minimum and maximum values of the earth's magnetic field (and f_H), respectively. The data from region 2, where the average value of f_H is 0.479 Mc/s, are suitable for observing the higher harmonics of f_H - the value of 12 f_H, for example, is 5.75 Mc/s which is still within the frequency response of the sounder and which falls near the upper limit of the lower portion of the frequency vs. time curve where the interpolation between frequency marks is more reliable (Fig. 2). The data from region 3, where the average value of f_H is 1.072 Mc/s, provides the best available opportunity for observing the resonance at f_H since the response of the sounder drops rapidly for frequencies below about 1.4 Mc/s (Molozzi, Fig. 8, 1963). Regions 4 and 5 were selected because the satellite's velocity vector and the earth's magnetic field vector were nearly perpendicular and nearly parallel, respectively. These conditions were investigated mainly to determine the presence or absence of resonances, thus the more convenient ionogram format was used rather than the amplitude vs. time format. In all of the above cases the limitation imposed on the size of the data region provided nearly constant nf_H frequencies, in any given region, and a uniform response could be assumed for the Alouette I sounder.

Method of analysis. A major portion of the analysis was centered on the investigation of the harmonic relation $f_n=nf_H$ as applied to the observed cyclotron harmonic resonances. The quantity B_R-B_C was measured for each cyclotron harmonic resonance on every ionogram of interest, where B_R is the magnetic field deduced from the frequency of the resonance and B_C is the computed field based on the GSFC(9/65) reference field (Hendricks and Cain, 1966). (In general, only one ionogram per pass was considered in any given region.) The measured quantity B_R-B_C should be constant for all the harmonics of f_H if they follow the $f_n=nf_H$ relationship. The field B_R was determined from the expression

$$B_R(\gamma) = \frac{1000}{27.994} \frac{f_n(kc/s)}{n} \approx 36 \frac{f_n(kc/s)}{n}$$

$$n = 1, 2, 3, \ldots\ldots \qquad (1)$$

This analysis is limited by the accuracy to which f_n can be determined since each 1 kc/s error in f_n introduces an error of approximately $(36/n)\gamma$ in B_R.

There are five main sources of error that limit the accuracy of the above procedure. They are the uncertainties in the frequency marks, the interpolation between frequency marks, the selection of the center frequency of the resonance, the orbit, and the magnetic activity. These uncertainties are discussed below:

(1) Frequency marks. Frequency marks are present on the telemetered data at 0.5, 1.5, 2.5, ---- 11.5 Mc/s and also at 2.0 and 7.0 Mc/s. They appear as heavy vertical lines on the ionogram format and as rectangular pulses on the amplitude vs. time format (Figure 1). Pre-launch tests indicated that the same correction term of -2 ± 1 kc/s should be applied to

each of the 12 non-integer frequency marks and a correction term of -8±4 kc/s to the two integer frequency marks (E. A. Walker, private communication, 1965). The latter frequency marks were intended for identification rather than for measuring and thus were not used in the present analysis. An attempt was made to check the frequency mark correction term by observing the WWV standard time signal on 10.0 Mc/s as transmitted from Greenbelt, Maryland and received on the Alouette sounder as it passed overhead. A clear signal was recorded on eleven occasions and the correction term for the non-integer frequency marks was estimated to be -2±10 kc/s; the large error resulted from the uncertainty in the interpolation between the frequency marks which are not linearly spaced with respect to time as is evident from Fig. 2. In spite of the limitation of the above test, the results indicate that there is no reason to assume that a frequency shift has taken place since launch; hence, the pre-launch values were used in this analysis.

(2) Interpolation. A 3rd degree interpolation was used between frequency marks. This procedure was considered accurate to better than 1 kc/s except in the frequency range above 5.5 Mc/s where it is difficult to interpolate with accuracy (see Fig. 2). A third degree extrapolation was used for frequencies below 1.5 Mc/s when the 0.5 Mc/s frequency marker was not present.

(3) Selecting the center frequency. The determination of the center frequency for any given resonance was assisted by measuring the duration of each pulse (from the amplitude-time format) in the resonant series, passing 2nd and 3rd degree curves through the values adjacent to the peak value to obtain estimates for the peak time, and then interpolating between

the frequency marks to obtain the corresponding frequency. The resonant duration is defined as the time interval between the onset of the transmitter pulse and the point where the resonant signal has decayed to the noise level prior to the pulsed disturbance. This quantity could usually be measured to an accuracy of $\pm$ 0.1 msec on all resonances except for some of the resonances associated with f_N and f_T which often displayed large amplitude fluctuations. The duration of each resonant pulse was measured rather than its amplitude, since amplitude shaping and limiting circuits were employed in the Alouette I receiver (Molozzi, P. 432, 1963). Also, possible uncertainties introduced by the AGC action of the receiver were minimized by this technique since the transition from the resonant signal to the background noise level was, in general, easy to distinguish. (The background noise level was not significantly altered during or following a series of large resonant pulses which indicates that the AGC action had very little effect on the above type of measurement.) The uncertainty involved in the above procedure depends on the nature of the data and varies from a few kc/s up to the frequency interval between pulses - which varies from 15 to 20 kc/s over the frequency range of the sounder. The scatter in the data, however, indicate that the average error was approximately $\pm$ 4 kc/s (see Appendix). If the data are scaled in the ionogram format, the corresponding error is approximately $\pm$ 20 kc/s.

(4) Orbit. Errors in the determination of the orbit produce effective errors in the calculated field B_C. The position accuracy of the Alouette I satellite at any given time was taken as $\pm$ 4 km along its orbital path and $\pm$ 0.5 km in altitude. These position errors give rise to errors in B_C of

16, 5, and 10γ in regions 1, 2, and 3, respectively. [It has been recently called to the author's attention that the position errors may be as high as ± 10 km in the horizontal direction and ± 4 km in the vertical direction (J. W. Siry, personal communication, 1967); the corresponding errors in B_C are 81, 28, and 70γ in regions 1, 2, and 3, respectively. These values are upper limits, however, and the relatively low scatter of the data points in the present analysis (see Appendix) indicates that the former values are reasonable estimates of the probable errors.]

(5) Magnetic activity. The data were restricted to periods of low magnetic activity in order that B_C would provide a consistent estimate of the true field. Only data corresponding to time intervals when the geomagnetic planetary 3-hr range index K_p and the Fredericksburg 3-hr range index K_{Fr} were less than 2 were considered. In addition, for the data from the low latitude region, i.e., the AGA-SNT data of region 2, the hourly values of the equatorial D_{st} (the average magnetic storm field over all longitudes) as given by Sugiura and Hendricks (1966) were restricted to absolute values less than 20^{γ} and these values were subtracted from the computed B_C values. Similar corrections are not available for the solar quiet day variation field Sq at the satellite's altitude of 1000 km; they are considered to be of the order of 10^{γ} (J. C. Cain, personal communication, 1967).

Frequency shift with n. The results of the above difference field analysis for the three main regions under investigation are presented in Fig. 3a (each point represents a weighted average - see Appendix). A linear shift is observed in the value of B_R-B_C (or in B_R since B_C is merely a reference level) with increasing harmonic number when n ≥ 4 in the low-latitude region (AGA-SNT), and this shift is offset between the 7th and 8th

harmonics. This observed shift in B_R implies a deviation in the resonant frequency from the harmonic relation $f_n=nf_H$; the maximum frequency displacement is $-0.6 \pm 0.1\%$ between $4f_H$ and $12f_H$. As a result of the restrictions imposed on the data collection procedure as described in the introduction, the resonances at the higher harmonics were observed very infrequently. This limitation is compensated for by the higher accuracy of the magnetic field determinations based on these resonances (see Appendix). In the two other regions the value of B_R associated with $2f_H$ is significantly higher than the remaining values when the points with large uncertainties pertaining to single observations are ignored.

In order to determine whether the shift in B_R with n observed in the low-latitude data was real - and not caused by a faulty choice of the frequency mark correction term - the data were plotted for all possible values of this term in Fig. 4. The results indicate that the observed shift is present in the data rather than being introduced during the process of analysis.

Frequency shift with N. The above data were restricted into groups with high and low electron density N and the results are presented in Fig. 3b (except for the BPO station where the available data were limited). This data division was possible because the data were fairly well distributed in local time (Fig. 5) which caused a considerable variation in electron density as can be seen from an inspection of Fig. 6 where the distribution of the plasma frequency in local time is presented. Also presented in this figure is the distribution of the upper hybrid frequency f_T in local time. The value of f_T, with respect to nf_H, is of major importance in dispersion theory; the relative positions of these frequencies are illustrated in Fig. 7.

Positive frequency shifts are observed with an increase in N at $2f_H$ ($+.19\pm.06\%$) in the high latitude region and at $3f_H$ ($+.4\pm.2\%$) in the low latitude region. The resonance at n=2 is the only nf_H resonance observed to be dependent on N in the high-latitude region, whereas it is the only major nf_H resonance observed to be independent of N in the low-latitude region. Local conditions were considerably different in these two cases in that $f_T < 2f_H$ for all values of N in the former but $f_T > 2f_H$ for all values of N in the latter (Fig. 7). The direction and magnitude of the frequency shifts observed at 4, 5, and $6f_H$ in the low latitude region suggests that they may be the result of the diurnal variation in Sq rather than the variation in N. The resonances n=7 and 8 in this region seem to represent a transition between low and high harmonics. In both cases they agree with the lower harmonics when N is low. When N is high, however, the resonance at n=7 has unique properties in that it agrees very well with the other high N resonances (with $n < 7$) only if the maximum observed resonance, n_{max}, recorded on the same ionogram satisfies the condition $n_{max} \geq 9$. When $n_{max} < 9$ the n=7 resonances for high N are shifted to higher frequencies. All of the resonances (high and low N) for n=8 were observed when $n_{max} \geq 9$; the high N values agree very well with the higher harmonics and the low N values agree very well with the lower harmonics. The resonances for $n \geq 9$ were all averaged together because of the limited data available for these resonances; also, the three values from the low N group (2 values for n=9 and one value for n=10) were consistent with the remaining 14 values from the high N group.

Frequency of occurrence and durations. The frequency of occurrence of a given nf_H resonance in each region, and the time durations of the nf_H resonances in each region are presented in Fig. 8 and 9 respectively. The transition frequency of 4.7 Mc/s, which marks the approximate frequency region of the change-over from the domain of the long antenna to the domain of the short antenna, is indicated on both figures. Two factors can influence the above results. First, the number of resonances observed is somewhat dependent on ionospheric conditions since the receiver can be desensitized by interference from ground transmitters; this condition, in general, prevents the observation of cyclotron harmonic resonances at frequencies greater than f_{max} - the critical frequency of the F-layer (Lockwood, 1965). An indication of the importance of this effect on the relative number of cyclotron harmonic resonances observed (Fig. 8) can be obtained from the average value of the quantity $f_{max}-(nf_H)_{max}$. This quantity, expressed in units of $\overline{f}_H$, represents the average number of additional cyclotron harmonic resonances that could have been observed with $f < f_{max}$ and is presented, together with $\overline{f}_H$, for each region in Table 3. The values indicate that ionospheric conditions were not a major factor in limiting the number of higher harmonics observed. Second, strong resonances often overlap making resolution impossible - in such cases neither resonance is included in the data. The cyclotron harmonic resonances are free from this contamination effect when $n \geq 2$ for the data from the mid and high-latitude regions and when $n \geq 4$ for the data from the low-latitude regions. The observational conditions for overlap are summarized in Table 4.

The high frequency of occurrence and long durations of the nf_H resonances observed in the region where the satellite motion is approximately

parallel to the direction of the earth's magnetic field (QUI data of Fig. 8 and 9) suggest a possible dependence of resonance duration on the angle β between the satellite velocity vector $\vec{V}_s$ and the earth's magnetic field vector $\vec{B}$. This dependence is evident in Fig. 10 where the maximum value for the duration of a given resonance is plotted against cos β; it increases with increasing cos β for f_N and nf_H with $n \leq 3$ but decreases for f_T. The minimum value (of this maximum duration) for f_T occurs when cos β=1 and is equivalent to the critical time T_L (see Table 1). The resonance at $2f_H$ appears to be a special case in that it is more difficult to establish a definite trend. The electron plasma resonance f_N was not definitely identified on any one of the 47 ionograms from region 4 (RES data) where cos $\beta \approx 0$. In several cases the calculated value for f_N was greater than the observed f_z exit frequency and there were no other resonances observed in the vicinity to obscure the identification of f_N - yet it was not observed. The f_H resonance is one of the strongest resonances observed in the high-latitude regions in spite of a -40 db sounder response at f_H. The lack of observations of the resonance at f_H in the low-latitude data is caused by instrumental limitations. The observed trends for the resonances at $2f_H$, $3f_H$, etc., are real, however, since instrumental effects would produce the opposite trends.

The duration of each resonance is plotted against the ratio f_N/f_H in Fig. 11. The theoretical curves for the relative duration of a given resonance as computed from the electrostatic approximation by Fejer and Calvert (Fig. 4, 1964) are presented for comparison with the observed data points. The vertical adjustment of these curves is arbitrary; they are

presented as given by Fejer and Calvert, i.e., in agreement with their observations (which are not reproduced here). The data points presented in Fig. 11 represent individual measurements - not averages - and it should be kept in mind that there is a considerable variation in the duration values (about 50% around the mean) as a function of satellite spin. There is fair agreement between the present observations and the electrostatic approximation for the resonances at f_H, $3f_H$, and $4f_H$; the agreement is uncertain for the resonances at f_N and f_T and it is poorest for the resonance at $2f_H$.

Over-all structure of resonances. A typical resonance is composed of approximately 10 pulses of the form shown in the lower format of Fig. 1 and the duration of each pulse is plotted against frequency in Fig. 12a. The example of Fig. 12a, which is typical, illustrates that the shape of the curve cannot be determined from one resonance alone, because the build-up and decline around the maximum is often not uniform. For this reason, all the observations of a given resonance from a given station were normalized in duration and frequency. The normalization in duration eliminated the considerable variation in peak-duration resulting from satellite spin; the normalization in frequency (a slight linear shift of the individual points) eliminated the already small variation in center frequency for a given set of observations of the same cyclotron harmonic resonance. The normalized values are presented in Fig. 12b-i. In Fig. 12 b and d the available observations of the $2f_H$ resonance from two different data regions are presented. In all the examples presented in Fig. 12 most of the points fall within $\pm$ 100 kc/s of the center frequency. The points

outside this range that appear in the f_H resonance from the GFO data and the $3f_H$ resonance from the AGA-SNT data in Fig. 12c and e, respectively, resulted from the overlapping of the above resonances with the f_T resonance (see Table 4 and Fig. 7). This overlapping contamination of the $3f_H$ resonance is not present in Fig. 12f where only selected resonances are considered. The resonances $4f_H$, $5f_H$, and $6f_H$ are presented in Fig. 12g, h, and i, respectively. The frequencies of the individual resonant pulses associated with the higher harmonics are also well within $\pm$ 100 kc/s of the center frequency. Occasionally one of these higher harmonic resonances shows a double peak structure on an ionogram; this splitting occurs when the resonant radiation received on the pulse near the center of the resonance is of lower amplitude and shorter duration than the outside pulses.

Fine structure of resonances. Large amplitude fluctuations, which occasionally become periodic, were observed during the decay of some resonances. These fluctuations often accompanied the f_T resonance in the high latitude region (GFO) and the f_N resonance in the low latitude region (AGA-SNT). They became periodic on 45% of the observed f_T resonances in the above high-latitude region (but never in the above low-latitude region) and on 22% of the observed f_N resonances in the low-latitude region (but never in the high-latitude region). Examples of these conditions are presented in Fig. 13; it is apparent that the frequency of the fluctuations is different for each resonance ($1.9 \pm .1$ kc/s for the f_N resonance and $2.7 \pm .1$ kc/s for the f_T resonance), and that the periodic fluctuations are more prominent near the end of the

resonant signal than near the beginning. A preliminary investigation of the fluctuations indicates a frequency variation for the same resonance from one region to another. They appear as a "fringe-pattern" on the plasma resonances observed by the Explorer 20 fixed-frequency topside-sounder (Calvert and Van Zandt, 1966).

A decaying signal of short duration is often observed at f_X, the exit frequency for the extraordinary wave, on the amplitude-time format but is not obvious on the ionogram format where it appears as part of the extraordinary wave reflection trace. The record presented in Fig. 1 is a good example of this condition; the last three pulses from the f_X amplitude-time trace of this figure show the progressive separation of the pulse into two components, i.e., a decaying signal and an echo-return with increasing time delay on each succeeding pulse. The decaying signal has the appearance of a short duration resonance but can also be interpreted as a signal generated by the frequency side bands of the transmitted pulse. Calvert and Van Zandt (1966) conclude that resonances are not observed at f_X or f_Z on the Explorer 20 fixed-frequency sounder records and that the apparent resonances observed at these frequencies on the Alouette I ionograms are caused by ionospheric irregularities.

Antenna orientation. It was observed that strong resonances were received on the long antenna at f_N, f_T, $2f_H$, and $3f_H$ when resonances at the high harmonics of f_H were observed on the same ionogram in the low-latitude data. The latter condition implies that the short antenna (which is perpendicular to the long antenna) was nearly parallel to the earth's magnetic field at the time of observation (Lockwood, 1965). Thus, even

after allowing for the satellite spin between the times when the low and high harmonics are received, the observations indicated that resonances of long duration are received at f_N, f_T, and the lower harmonics of f_H when the radiating antenna is far removed from the parallel configuration which is so necessary for the observation of resonances at the higher harmonics of f_H. Two cases where long duration resonances were observed were investigated in detail. The results fully support the above hypothesis in that the long antenna was observed to make an angle of 101^o with the magnetic field direction during the time of observation of resonances of extremely long duration (f_T, f_H, and $2f_H$ on one GFO ionogram and $3f_H$ on one AGA ionogram - the corresponding angles between the long antenna and the direction of satellite motion were 47^o and 85^o respectively).

Interpretation

Magnetic contamination. Alouette I was designed for ionospheric - not magnetic - measurements and pre-launch magnetic tests were not conducted. The fairly low values of the quantity $|B_R - B_C|$, however, indicates that the magnetic contamination was not large (Fig. 3a). The concern of magnetic contamination thus centers around a possible small field which could give rise to the observed shift and/or offset so clearly observed in the low-latitude data (AGA-SNT) of Fig. 3a. Such a magnetic field could originate in the permanent or induced field of the satellite body or its antennas.

Pre-launch magnetic tests were conducted on the similar Alouette II satellite; the results indicated that the permanent field was greater than the induced field by approximately a factor of 5. The maximum radial

component of the permanent field in the equatorial plane of the satellite was 100γ at 1.5m and less than 15γ at 3m; the maximum radial component along the spin axis was 5γ at 2m (C. A. Harris, personal communication, 1967). The antenna elements on Alouette I must also be considered as a possible source of magnetic contamination since they were composed of spring steel. A 24 ft. section of this material was obtained from the same stock as used in Alouette I (courtesy De Havilland Aircraft of Canada, Ltd.) and magnetic tests indicated that the permanent field was greater than the induced field by more than a factor of 10. The permanent field was only a few gammas at a radial distances of several meters from the antenna element (6γ at 2m) but was very large near the antenna element (450γ at 15 cm).

Frequency shifts. The frequencies of the nf_H resonances observed in the low latitude region (Fig. 3a, AGA data) follow the empirical relationship

$$f_n = n \frac{f_4}{4} [1 - \epsilon(n)]$$

where $\epsilon(n) = (n-4)(.09 \pm .02)(10^{-2})$ and where $4 \leq n \leq 7$. The resonances with $n > 7$ agree with this expression if the reference field B_C in Fig. 3a is shifted by +47γ for each of these resonances.

This negative frequency shift with increasing harmonic number n is not predicted by any of the existing theoretical treatments of the Alouette plasma resonance problem. It cannot be explained in terms of the AGC action of the receiver (no scaling corrections were made for the AGC) since shifts opposite to the observed shifts would be expected if this action influenced the results. It is difficult to explain in terms of magnetic

contamination from a permanent field on a spinning satellite such as Alouette I because of the consistency of the data. An induced field, which would not reverse sign as the satellite spins, would appear to be a more likely cause of the frequency shift at the higher harmonics; the measurements discussed under 'magnetic contamination', however, (see above) indicate that this field is much weaker than the permanent field. An investigation of the plasma resonances observed by the Alouette II satellite, where non-magnetic Be-Cu antennas are used, should determine whether this frequency shift is a natural phenomenon or simply the result of magnetic contamination. The positive frequency offset observed for the resonances with $n \geq 8$ is attributed to an antenna orientation effect since the higher harmonic resonances are only observed when the radiating antenna is nearly parallel to $\vec{B}$ (Lockwood, 1965) and this orientation restriction appears to be the cause of the low frequency of occurrence of the resonances with $n \geq 8$ in the AGA-SNT data (Fig. 8) since ionospheric conditions, on the average, would have allowed 7 more nf_H resonances to be observed per ionogram (Table 3). Again, an investigation of Alouette II data should help to determine whether this offset is due to antenna magnetic field contamination or to other causes.

The dispersion theories do predict relatively large frequency shifts with variations in the electron density N for the nf_H resonances with $n < 4$, i.e., in the frequency range of the upper-hybrid frequency f_T. The shifts expected for the longitudinal waves with $\vec{k} \cdot \vec{B} = 0$ (the so-called Bernstein modes) can be visualized by inspecting the dispersion curves based on the electrostatic approximation with $\theta = \pi/2$. Two sets

of dispersion curves are presented in Fig. 14; the slope of each curve is proportional to the group velocity. The cases presented are pertinent to the Alouette I low-latitude data (AGA-SNT), in that the value of f_T sweeps through the value of $3f_H$ (see Fig. 7). The shape of the dispersion curve for the longitudinal wave associated with $3f_H$ changes drastically during the above change in f_T. The corresponding change expected in the observed frequency of the resonance at f_3, based on matching V_s to $|V_g|$ in the region of small k, is from $f_3 > 3f_H$ (positive slope) to $f_3 < 3f_H$ (negative slope) as f_T increases. The observed frequency shift is in the opposite direction (Fig. 3b). The observed shift, however, is in the same direction as interpreted from the curves given by Shkarofsky (Fig. 6, 1966), which correspond to the matching of non-longitudinal wave group velocities to the satellite velocity, near the critical condition of $f_T \approx nf_H$. The similar frequency shift observed for the n = 2 resonance in the high-latitude data of Fig. 3b is more difficult to interpret because the matching conditions for longitudinal and non-longitudinal waves both appear to be important (Shkarofsky and Johnston, 1965; Shkarofsky, P. 62, 1966) and the critical condition $f_T \approx f_n$ is never satisfied (Fig. 7). The observed frequency shift for this resonance is in the same direction as predicted by the electrostatic approximation where positive shifts are expected with an increase in N when $f_T \neq f_n$ (Fejer and Calvert, eq. 30, 1964). The observed shifts for the n = 4, 5, and 6 resonances are in the opposite direction but may be the result of a variation in the Sq field (see "Observations").

Magnetic field reference level. The observed deviations of the nf_H resonant frequencies from their harmonic values introduces the problem of determining the resonance of minimum frequency shift for magnetic field calculations. A comparison between the GSFC(9/65) reference field used in this work and the recent GSFC(12/66) reference field, which includes data from the OGO-2 satellite, (J. C. Cain, personal communication, 1967) indicates that the zero levels in Fig. 3 should be modified as follows: lowered by 3γ in region 1 (BPO), lowered by 9γ in region 2 (AGA-SNT), and raised by 1γ in region 3 (GFO). The probable error associated with this field in the above regions is $\pm$ 20γ; extrapolated rocket measurements of the magnetic field over Wallops Island, Virginia (38°N, 75°W) during periods of low magnetic activity (Davis, et al, 1965) are consistent within these error limits. The consistent resonant frequencies are f_3 when $f_T < f_3$ (GFO, BPO, and low N AGA-SNT data - see Fig. 7) and f_2 when $f_T > f_2$ (AGA-SNT data).

Wave group velocity. The long time durations observed for some of the plasma resonances has been attributed to plasma waves with group velocities matched to the satellite velocity (Shkarofsky and Johnston, 1965). It is only necessary to invoke this matching requirement when the resonant duration exceeds the time T, since the resonances of shorter duration can be attributed to the excitation of plasma waves of nearly zero group velocity around the antenna. In this case the resonant duration is determined by the time required for the antenna to move through the region of original excitation (Sturrock, 1965). This line of reasoning can be extended to include the resonances of longer duration by assuming a region of original excitation larger than the dimensions of the antenna.

If it is assumed that a resonance of long duration (i.e., greater than T) corresponds to the above matching between wave group velocity and satellite velocity, then an inspection of Figure 9 indicates that only the nf_H resonances at n = 2, 3, and 4 in the low latitude regions (AGA-SNT and QUI) and those at n = 1 and 2 in the high latitude regions (RES and GFO) satisfy this condition. Similarly, the resonances at f_N and f_T satisfy this condition in the low and high latitude regions, respectively (Figure 10). If these plasma waves have a preferred direction of propagation with respect to $\vec{B}$ then one would expect the observed resonant duration to be dependent on the angle β between $\vec{B}$ and $\vec{V}_s$; the long and short duration of a given resonance being observed when the satellite travels parallel and perpendicular to the propagating plasma wave, respectively. The maximum duration of the f_N resonance is greatest when the satellite travels nearly parallel to $\vec{B}$; the resonance is not observed when the satellite travels nearly perpendicular to $\vec{B}$. Thus $\vec{V}_g$ is approximately parallel to $\vec{B}$ for the plasma wave associated with f_N and the component of resonant radiation with $\vec{V}_g \approx 0$ is negligible. The maximum duration of the f_T resonance is greatest when the satellite travels nearly perpendicular to $\vec{B}$ and drops to the value of T_L (see Table 1) when the satellite travels nearly parallel to $\vec{B}$. Thus $\vec{V}_g$ is approximately perpendicular to $\vec{B}$ for the plasma wave associated with f_T, and the component of radiation with $\vec{V}_g \approx 0$ is significant. The trend of the $3f_H$ data indicates that the group velocity of the plasma wave associated with this resonance is directed approximately parallel to $\vec{B}$ rather than perpendicular to $\vec{B}$ as would be expected from the theoretical work of Fejer and Calvert (1964) which is based on the electrostatic

approximation. The resonances at $n \geq 5$ associated with the waves of nearly zero group velocity attain their maximum durations when the satellite travels nearly parallel to $\vec{B}$. This is to be expected since the favorable antenna orientation for the excitation of these waves is parallel to $\vec{B}$ (Lockwood, 1965) and thus the antenna requires a longer time to move through the region of original excitation. The resonance at $n = 4$ seems to represent a transition between the conditions of $\vec{V}_g \approx \vec{V}_s$ and $\vec{V}_g \approx 0$ (since durations in excess of T_L are not common), with $\vec{V}_g$ directed mainly along $\vec{B}$. The plasma wave associated with $n = 2$ is not restricted to either of the parallel or perpendicular propagation conditions. The wave associated with f_H is observed when the satellite travels nearly perpendicular to $\vec{B}$; instrumental limitations prevent its observation when the satellite travels nearly parallel to $\vec{B}$.

If it is assumed that the resonances of long duration simply correspond to a larger region of original excitation, then the data presented in Figure 10 can be interpreted in terms of the shape of this excitation region. The electron plasma resonance at f_N corresponds to a narrow region elongated along $\vec{B}$, the upper-hybrid resonance corresponds to a relatively wide (dimensions of the order of the long antenna) region elongated perpendicular to $\vec{B}$, the $2f_H$ resonance corresponds to a roughly symmetrical region with dimensions slightly larger than the long antenna, and the nf_H resonances with $n \geq 3$ correspond to narrow regions (smaller dimentions associated with higher n values) elongated along $\vec{B}$.

The earlier assumption of traveling waves keeping up with the satellite appears to be more consistent with the data for the following reasons: (1) the long time durations associated with the f_N and f_T resonances would require elongated dimensions of the order of three antenna lengths - or more - for the original excitation region, (2) the lack of observations of the f_N resonance in the RES data - satellite motion approximately (within 2^o) perpendicular to $\vec{B}$ - implies dimensions of the order of 5 m or less in the direction perpendicular to $\vec{B}$ (the satellite velocity is 7.3 m/msec and a resonance of the order of 0.7 msec can be detected), and (3) the direction of the frequency shift of the $3f_H$ resonance near the critical condition of $3f_H \approx f_T$ agrees with the theoretical work based on matching $\vec{V}_g$ to $\vec{V}_s$.

Region of original excitation. The lack of serious magnetic contamination from the spring steel antennas definitely indicates that the excitation region is not confined to the sheath region surrounding them. Thus, from the point-of-view of the present discussion it is fortunate that the antenna elements were not composed of a non-magnetic material - as they would have been if the experiment was designed for measuring the magnetic field by observing cyclotron-harmonic plasma resonances. The observed restricted time durations of the resonances indicates that this excitation region does not extend beyond several antenna lengths from the satellite. The maximum observed time duration for the resonances at n=5 and 6 are equal to T_L, the shorter duration times for the resonances at $n > 6$ can be attributed to a smaller resonant region or to the lack of optimum antenna orientation (Figures 9 and 10). In

the high-latitude regions the short time durations for the higher nf_H resonances indicates that the excitation region has a cylindrical geometry around the antenna. When the antenna is oriented approximately parallel to $\vec{B}$, for favorable excitation of these resonances, the satellite motion is approximately perpendicular to the antenna and quickly moves through the resonant region which is of the order of 7m or less in radius for a resonance persisting for less than 1 msec.

The agreement of the observed value of the electron plasma resonant frequency f_N with the calculated values (based on the nf_H resonances, the f_T resonance, and the exit frequencies f_x and f_z) indicates that the excitation region associated with this resonance is also not confined to the antenna sheath region.

Spectral response curves. The wide frequency range over which a given nf_H plasma resonance is observed (Figure 12) is attributed to the reception of side-bands of the transmitted pulse within the bandwidth of the receiver. A quick inspection of the nf_H resonances observed by Alouette II indicates that they cover a shorter frequency interval (80 ± 10 kc/s) than those observed by Alouette I. This difference is to be expected since the overall receiver bandwidth on Alouette II at the 20 db point is considerably less than on Alouette I [73 kc/s compared with 115 kc/s (C. A. Franklin, personal communication, 1967)]. The nf_H resonances observed by Alouette I appear slightly wider than expected on the basis of bandwidth considerations alone and the non-uniformity in the magnetic field near the antennas may be responsible - especially for the higher harmonics where this type of broadening would be greatest and where less resonant energy would be expected to be excited by the

low energy components of the transmitted frequency spectrum. A broadening would be expected if the antenna elements were oppositely directed magnetic dipoles and such a broadening could be responsible for the splitting observed on some of the higher nf_H resonances. The main source of broadening, however, are the instrumental effects mentioned earlier; other broadening mechanisms (Heald and Wharton, P. 274, 1965) are insignificant in the present problem.

Natural spectral width of nf_H resonances. An estimate of the natural spectral width of the nf_H plasma resonances can be obtained from these curves. The anomalous resonant pulses of short duration observed within a given resonant series of pulses (Fig. 12a) are attributed to a condition when the resonant frequency in the medium coincides with a null-point in the frequency spectrum of the transmitted pulse. The large scatter observed on the normalized spectral response curves of Figures 12 b-i is also attributed to this condition. These observations imply a natural spectral width of less than 10 kc/s for the nf_H resonances.

Energy requirements for resonance excitation. An estimate of the energy required to excite the resonant radiation can also be obtained from the above observations. Frequency side lobes as high as the seventh are observed to be important; the corresponding transmitted energy is down by 27 db from the main spectral component of the 100 watt, 100 μsec pulse. Thus a transmitted energy of less than 0.2 w is sufficient to initiate the plasma resonances observed at f_N, f_T, and nf_H with n values up to 5; slightly more energy may be required for the higher n values where only three or four frequency side lobes initiate the observed plasma resonances.

describe the resonance. The latter situation appears more relevant to the present observations of the f_T resonance in the high latitude GFO data region since the ionospheric parameters are such that the requirements (Deering and Fejer, 1965, eq. 77) of the electrostatic approximation are not very well satisfied and that the requirements (Fejer, 1966, eq. 34) of the cold plasma approximation are never satisfied for these data.

Cyclotron resonance magnetometer. The observed departure of the nf_H plasma resonances from a true harmonic relation complicated their application toward determinations of the total scalar magnetic field. The observed variation of resonant frequency as a function of the electron density, which is greatest for the resonances near $2f_H$ and $3f_H$, also must be considered. A comparison of the observations with a calculated reference field, and with theoretical predictions, indicates that when $f_T < 3f_H$ the $3f_H$ resonance gives the best value of the magnetic field, whereas when $f_T > 3f_H$ this resonance gives a value that is higher than the true field. Such comparisons are very sensitive to uncertainties in the absolute level of the reference field, however, and a combination plasma resonance and magnetometer experiment may be required to determine which resonances experience negligable frequency shifts. The magnetic field determinations based on the Alouette I cyclotron harmonic resonance frequencies are accurate to approximately 1% when the conventional ionogram data format is used. When the data is scaled in the receiver-output amplitude vs. time format the uncertainty is less than 0.5% which is of the order of the uncertainty introduced by the observed frequency shifts with harmonic number and electron density.

(This power estimate is an upper limit because a perfectly rectangular pulse is assumed.)

f_N and f_T periodic amplitude fluctuations. Large periodic amplitude fluctuations are observed during the decay of the f_N and f_T resonances only when the satellite is moving nearly parallel to the propagation direction of the plasma waves associated with these resonances (Fig. 13); the fluctuations are smaller and of a non-periodic nature when these conditions are not satisfied. If these waves are considered to be longitudinal waves, as suggested by Fejer and Calvert (1964), the implications are that the strong periodic amplitude fluctuations are observed only when the observation point moves in nearly the same direction as the oscillations of $\vec{E}$. The theoretical work of Deering and Fejer (1965), which is based on the electrostatic approximation, indicates that large variations in the received field strength of the f_N and f_T resonances can be expected in the direction parallel to $\vec{k}$ for observational distances not linearly related to time. They also find that the wave numbers corresponding to a group velocity equal to the satellite velocity contribute substantially to the field. As pointed out earlier, the present observations support the hypothesis of matching wave group velocity and satellite velocity for these resonances; thus the propagation distance z satisfies the expression $z=V_s t$ and no amplitude fluctuations would be expected on the basis of Deering and Fejer (1965). In later work on the f_T resonance, Fejer (1966) indicates that the contribution from the cold plasma approximation probably dominates the above electrostatic contribution and that under certain conditions both approximations break down so that a solution of the complete set of equations is required to

Electron density resonance probe. The consistency of the electron plasma resonant frequency f_N with the other resonant frequencies implies that the f_N resonance is not restricted to the antenna sheath region and that reliable ambient electron densities can be determined to an accuracy of approximately 2% from a given Alouette I record.

Appendix

The ith ionogram, from a given region, provides the data to calculate the quantity $(B_R-B_C)_i$ for each resonance appearing on that ionogram. A weighted average of the data from all ionograms containing a given resonance was calculated from the following expression:

$$\langle (B_R-B_C) \rangle = \frac{\sum_i w_i (B_R-B_C)_i}{\sum_i w_i} \qquad \text{(A1)}$$

The corresponding error limit was taken as the standard deviation of the weighted mean

$$\Delta \langle (B_R-B_C) \rangle = \left[\frac{1}{\sum_i w_i} \right]^{\frac{1}{2}} \qquad \text{(A2)}$$

where the weight w_i for each measurement is given by

$$w_i = \left[\frac{1}{\Delta (B_R-B_C)_i} \right]^2$$

and $\Delta(B_R-B_C)_i$ is the estimated uncertainty associated with the ith observation (Brownlee, 1965). In the limiting case where there are N observations, each with the same uncertainty ΔX, the expression for the error reduces to the more familiar form of $\Delta X/N^{\frac{1}{2}}$.

The error limit, as determined from (A2), is almost entirely dependent on the estimated error associated with each resonant center frequency measurement. From (1) this error is given by

$$(\Delta B_R)_i(\gamma) \approx 36 \frac{(\Delta f_n)_i \text{ (kc/s)}}{n} \qquad \text{(A3)}$$

The relative value of $(\Delta f_n)_i$ from one measurement to the next is considered to be reliable, but the absolute value is somewhat questionable since it is based on a subjective observation. Only relative values are necessary

for determining the weighted average from (A1), whereas absolute values are required in order to determine the corresponding estimate of error from (A2). In an attempt to estimate these absolute values it was assumed that any bias introduced into the original estimate of $(\Delta f_n)_i$ was consistent from one measurement to the next of a given plasma resonance. The true weight of the ith measurement can then be expressed as kw_i where k is a constant for all measurements of the resonance under consideration. An objective estimate of k was obtained as follows: First, the standard deviation σ of the unweighted values of $(B_R-B_C)_i$ was calculated for the resonance. Second, the expected value of $<\Delta(B_R-B_C)>$ was calculated from the expression $<(\Delta B_R)> = .798\sigma$ which assumes a normal error distribution (Chapman and Bartels, 1962) and a statistical sample large enough to provide a reliable estimate for σ; these conditions were satisfied for the lower resonances. A comparison of the calculated and observed values of $<(\Delta B_R)>$ indicated that the average value of $k^{-\frac{1}{2}}$ was .6 for these resonances, which implies that the original estimates for $<(\Delta f_n)>$ (between 8 and 9 kc/s for most resonances) were too high by 3 or 4 kc/s in each case. The value of k for each of the higher resonances was determined by assuming that the average value of the original $(\Delta f_n)_i$ estimates for these resonances was also too high by 3 to 4 kc/s. This assumption appears reasonable since there was very little variation of $<\Delta f_n>$ from one resonance to the next, which implies that the amount of the original overestimate was nearly uniform for all of the resonances. The major exception to the above statement is for one of the two resonances at n=12 where Δf_n was 19 kc/s. This larger scaling uncertainty is the reason that the error bars associated with the n=12 entry in Fig. 3a is larger than one would expect from (A2) and (A3).

[If Δf_n was a constant for all resonances, then 2 observations of the 12th harmonic should yield the same accuracy in determining B_R as 72 observations of the 2nd harmonic; this result follows from the expression $\Delta B_{n_2}/\Delta B_{n_1} = (N_1/N_2)^{\frac{1}{2}}\, n_1/n_2$ where ΔB_{n_1} is the error associated with N_1 observations of the resonance at $n=n_1$ and ΔB_{n_2} is the error associated with N_2 observations of the resonance at $n=n_2$.]

Acknowledgments

I gladly acknowledge the encouragement and the many critical discussions received from T. L. Aggson throughout the course of this work. I am grateful to J. P. Heppner for helpful comments concerning satellite magnetic field contamination, to J. C. Cain and S. J. Hendricks for their assistance in matters pertaining to the earth's reference field, to J. A. Fejer, I. P. Shkarofsky, and T. W. Johnston for helpful discussions on theoretical aspects of the problem, and to J. E. Jackson and S. J. Bauer for their continued interest in this analysis and for many helpful comments. I am also grateful to K. Motomoora of De Havilland Aircraft of Canada, Ltd., for supplying a section of the Alouette I antenna material, and to G. E. K. Lockwood of the Defence Research Telecommunications Establishment for supplying Alouette I aspect information for several cases of interest.

This research was conducted -in part- while the author was pursuing a NAS-NRC Postdoctoral Resident Research Associateship supported by the National Aeronautics and Space Administration.

References

Aggson, T. L., J. P. Heppner, and N. C. Maynard, Test flight of a triaxial dc electric field payload (abstract), Trans. Am. Geophys. Union, 48 156, 1967.

Barrington, R. E., and Luise Herzberg, Frequency variation in ionospheric cyclotron harmonic series obtained by the Alouette I satellite, Can. J. Phys., 44, 987-994, 1966.

Bekefi, G., Radiation processes in plasmas, John Wiley and Sons, Inc., New York, 1966.

Brownlee, K. A., Statistical theory and methodology in science and engineering, John Wiley and Sons, Inc., p. 95, 1965.

Cain, J. C., Models of the earth's magnetic field, in Radiation Trapped in the Earth's Magnetic Field, edited by B. M. McCormac, pp. 7-25, D. Reidel Publishing Co., Dordrecht, 1966.

Cain, J. C. and S. J. Hendricks, The geomagnetic secular variation 1900-1965, NASA, Goddard Space Flight Center Rept. X-612-67-479, Sept. 1967.

Calvert, W., and G. B. Goe, Plasma resonances in the upper ionosphere, J. Geophys. Res., 68, 6113-6120, 1963.

Calvert, W. and T. E. Van Zandt, Fixed-frequency observations of plasma resonances in the topside ionosphere, J. Geophys. Res., 71, 1799-1813, 1966.

Chapman, S. and J. Bartels, Geomagnetism, Vol. II, p. 574, Oxford Univ. Press, London, 1962.

Crawford, F. W., A review of cyclotron harmonic phenomena in plasmas, Nuclear Fusion 5, 73-84, 1965.

Crawford, F. W., R. S. Harp, and T. D. Mantei, On the interpretation of ionospheric resonances stimulated by Alouette 1, J. Geophys. Res., 72, 57-68, 1967.

Davis, T. N., J. D. Stolarik, and J. P. Heppner, Rocket Measurements of S_q currents at midlatitude, J. Geophys. Res., 70, 5883-5894, 1965.

Deering, W. D., and J. A. Fejer, Excitation of plasma resonances by a small pulsed dipole, Phys. Fluids 8, 2066-2079, 1965.

Dougherty, J. P. and J. J. Monaghan, Theory of resonances observed in ionograms taken by sounders above the ionosphere, Proc. Roy. Soc., A, 289, 214-234, 1965.

Fejer, J. A., Excitation of the lower hybrid resonance by an antenna in the ionosphere, Radio Science, 1 (New Series) 447-455, 1966.

Fejer, J. A., and W. Calvert, Resonance effects of electrostatic oscillations in the ionosphere, J. Geophys. Res., 69, 5049-5062, 1964.

Fitzenreiter, R. J., and L. J. Blumle, Analysis of topside sounder records, J. Geophys. Res., 69, 407-415, 1964.

Heald, M. A., and C. B. Wharton, Plasma Diagnostics with microwaves, John Wiley and Sons, Inc., New York, 1965.

Hendricks, S. J., and J. C. Cain, Magnetic field data for trapped-particle evaluations, J. Geophys. Res., 71, 346-347, 1966.

Johnston, T. W. and J. Nuttall, Cyclotron harmonic signals received by the Alouette topside sounder, J. Geophys. Res., 69, 2305-2314, 1964.

Lockwood, G. E. K., Plasma and cyclotron spike phenomena observed in top-side ionograms, Can. J. Phys., 41, 190-194, 1963.

Lockwood, G. E. K., Excitation of cyclotron spikes in the ionospheric plasma, Can. J. Phys., 43, 291-297, 1965.

Molozzi, A. R., Instrumentation of the ionospheric sounder contained in the satellite 1962 Beta Alpha (Alouette), in Space Research IV, edited by P. Muller, pp. 413-436, North-Holland Publishing Co., Amsterdam, 1963.

Shkarofsky, I. P., Duration of cyclotron harmonic resonances observed by satellites, RCA Victor Research Report 7-801-44, Montreal, January 1966.

Shkarofsky, I. P., and T. W. Johnston, Cyclotron harmonic resonances observed by satellites, Phys. Rev. Letters, 15, 51-53, 1965.

Stix, T. H., The theory of plasma waves, McGraw-Hill, Inc., New York, 1962.

Sturrock, P. A., Spectral characteristics of type II solar radio bursts, Nature 192, 58, 1961.

Sturrock, P. A., Dipole resonances in a homogeneous plasma in a magnetic field, Phys. Fluids, 8, 88-96, 1965.

Sugiura, M. and S. Hendricks, Provisional hourly values of equatorial D_{st} for 1961, 1962 and 1963, NASA, Goddard Space Flight Center Rept. X-612-66-355, Aug. 1966.

Table 1. Notation

NOTATION	DESCRIPTION
f_N	Electron plasma resonant frequency
f_H	Electron cyclotron resonant frequency
$f_T=(f_N^2 + f_H^2)^{\frac{1}{2}}$	Upper hybrid resonant frequency
f_x	Exit frequency of the extraordinary trace
f_z	Exit frequency of the Z trace
f_n	Observed frequency of the plasma resonance near nf_H
N	Electron density
$\vec{B}$	Total intensity of the earth's magnetic field
B_R	Magnetic field deduced from f_n
B_C	Calculated reference field
f_{max}	Critical frequency of the F layer
T	Travel time corresponding to a satellite motion equivalent to the tip-to-tip antenna length
T_L=6.3 msec	Value of T for the long antenna (46m)
T_S=3.15 msec	Value of T for the short antenna (23m)
$\vec{V}_s$	Satellite velocity ($\lvert\vec{V}_s\rvert$ = 7.3 km/sec)
$\vec{V}_g$	Group velocity of plasma wave

Table 2. Locations of regions of Alouette I plasma resonance investigations

REGION	STATION*	GEOGRAPHIC COORDINATES LAT. RANGE	LONG. RANGE	DIPOLE LAT. RANGE	INCLINATION RANGE**
1	BPO	37.8 ± 1.2	-78.0 ± 1.5	49.2 ± 1.1	69.0 ± 1.0
2	AGA-SNT	-23.5 ± 1.7	-65.4 ± 2.6	-12.0 ± 1.6	-16.5 ± 2.5
3	GFO	57.0 ± 1.3	-98.4 ± 3.8	66.4 ± 0.7	80.5 ± 1.0
4	RES	80.2 ± 0.3	-97.8 ±16.7	84.5 ± 2.8	89.4 ± 0.5
5	QUI	-10.7 ± 1.5	-88.1 ± 1.5	0.2 ± 1.6	0.5 ± 2.7

*BPO: Blossom Point, Maryland; AGA: Antofagasta, Chile; SNT: Santiago, Chile; GFO: East Grand Forks, Minnesota; RES: Resolute Bay, N.W.T.; QUI: Quito, Ecuador.

**Range of the magnetic inclination at 1000 km as calculated from the GSFC(9/65) reference field (Hendricks and Cain, 1966).

Table 3. Average values of f_H and $\{f_{max} - (nf_H)_{max}\}$

Station	$\bar{f}_H$(Mc/s)	$\langle \{f_{max} - (nf_H)_{max}\} \rangle$
BPO	0.973	1.3 $\bar{f}_H$
AGA-SNT	0.479	7.3 $\bar{f}_H$
GFO	1.072	1.3 $\bar{f}_H$
RES	1.057	1.7 $\bar{f}_H$
QUI	0.536	5.8 $\bar{f}_H$

Table 4. Possible overlap of f_N and/or f_T resonances with nf_H resonances

Station	f_H	$2f_H$	$3f_H$	$4f_H$
BPO	f_N & f_T			
AGA-SNT		f_N	f_N & f_T	f_T
GFO	f_N & f_T			
RES	f_N & f_T			
QUI		f_N & f_T	f_N & f_T	f_T

Figure Captions

1. Data formats from a BPO record (pass 2354). The plasma resonances appear as stalactites on the ionogram format (top) - the heavy vertical lines are frequency markers which depend on time (sweep frequency sounder), and the horizontal lines are time markers (each marker represents 2/3 msec delay time). The resonances are each composed of a series of responses, which appear as 'zero time-delay echos' following the individual sounder pulses, in the receiver-output amplitude vs. time format (below). The 16 msec separation between pulses (off scale in the ionogram format) is indicated for the f_N resonance. See Table 1 for notation.
2. Frequency marks vs. time on Alouette I (BPO pass 1309, 03:47 UT).
3. Difference field vs. harmonic number (see Table 1 for notation). Each point represents a weighted average over the indicated number of observations. All data from the three main data regions are presented in (a) and restricted data groups from two of these regions are presented in (b). The low N group corresponds to $f_N < 1.15$ Mc/s ($f_T < 1.24$ Mc/s) in the AGA-SNT data (low-latitude) and to $f_N < 0.44$ Mc/s ($f_T < 1.16$ Mc/s) in the GFO data (high-latitude); the high N group corresponds to $f_N > 1.37$ Mc/s ($f_T > 1.45$ Mc/s) in the AGA-SNT data and to $f_N > 0.73$ Mc/s ($f_T > 1.29$ Mc/s) in the GFO data (see Fig. 6). The difference between the average values of low N and high N is approximately a factor of 2 in the AGA-SNT data and 8 in the GFO data.
4. Difference field vs. n for various frequency-mark correction terms.
5. Data distribution in local time for the main data regions.

6. Variation of the electron plasma frequency f_N and the upper-hybrid frequency f_T with local time. The electron density N (cm^{-3}) can be obtained from the expression $N = (10^6)f_N^2/81$. [Calculated values - based on the other resonant frequencies observed on the same record - indicate that the observed resonant frequency was either beyond the frequency response of the sounder or was questionable due to the overlapping of a neighboring resonance (see Table 4).]
7. Relative positions of the observed range of the nf_H resonant frequencies with respect to the observed range of the upper-hybrid resonant frequency.
8. Frequency of occurrence of the nf_H resonances in each region (total number of ionograms: BPO, 13; AGA-SNT, 46; GFO, 40; RES, 47; QUI, 30).
9. Average and maximum time durations of the nf_H resonances observed in each region. The frequency domain of the short antenna is indicated by SA; the parameters T_L and T_S are defined in Table 1.
10. Maximum observed resonant time duration vs. cos β where β is the angle between the satellite velocity vector $\vec{V}_S$ and the earth's magnetic field vector $\vec{B}$. Straight lines are used to connect the values at each station for a given resonance. The observational limit is between 15 and 16 msec
11. Time duration of each resonance vs. f_N/f_H.
12. Normalized spectral response curves. The vertical scales are linear from zero up to the peak duration in each case.
13. Examples of the periodic amplitude fluctuations occasionally observed during the decay of the f_N and f_T resonances. Top: f_N resonance ($f_n = 1.33 \pm .01$ Mc/s) from SNT pass 4768 (16:49:06:35 UT). Middle: f_T resonance ($f_T = 1.37 \pm .02$ Mc/s) from GFO pass 5300 (15:06:11.77 UT). Bottom: 1 kc/s time code signal.

14. Dispersion curves in the electrostatic approximation; $k_\perp$ is the wave number in the direction perpendicular to $\vec{B}$ and R is the electron cyclotron radius (adapted from Crawford, 1965).

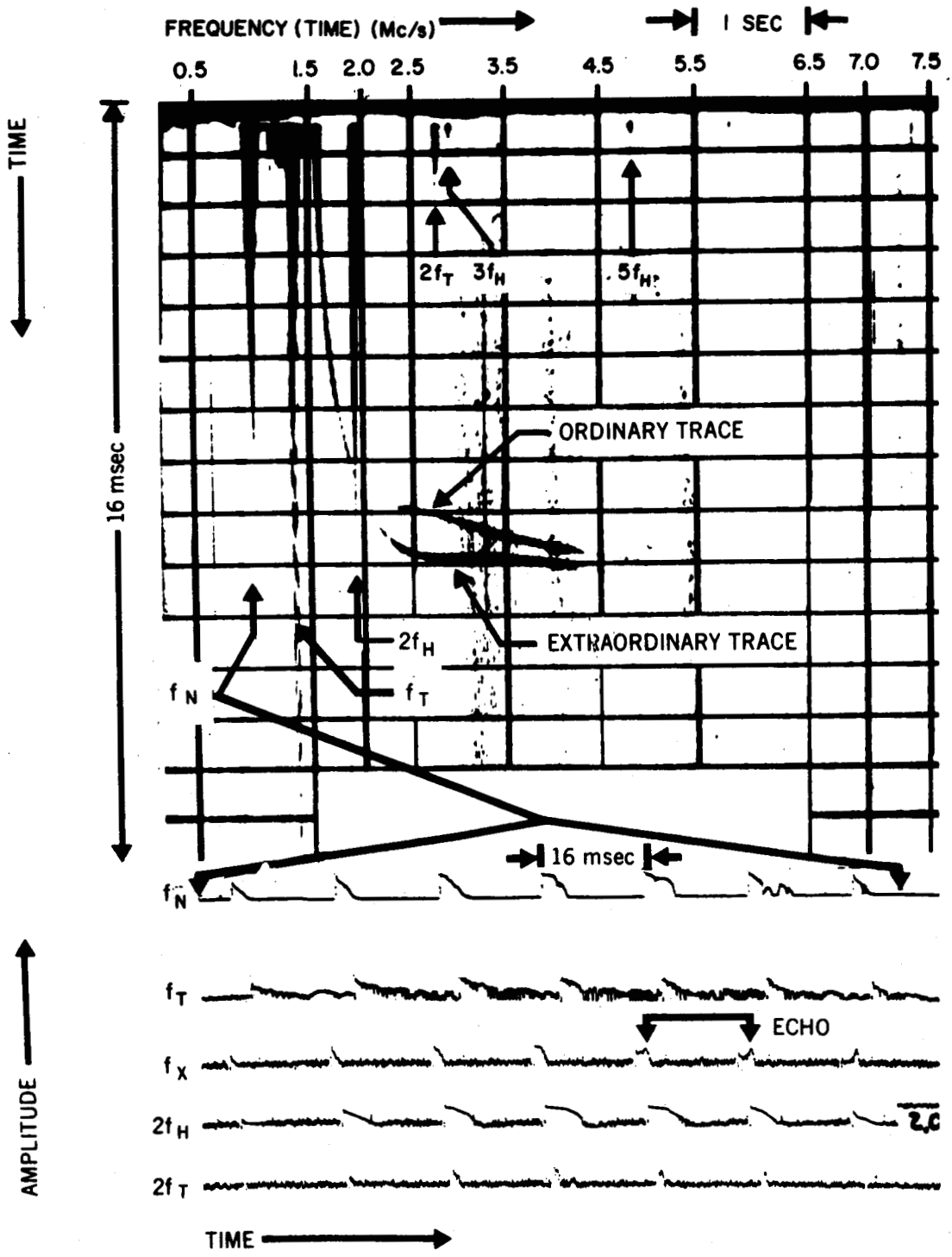
FREQUENCY (TIME) (Mc/s)
1 SEC
0.5
1.5
2.0
2.5
3.5
4.5
5.5
6.5
7.0
7.5
TIME
16 msec
$2f_T$ $3f_H$
$5f_H$
ORDINARY TRACE
$2f_H$
EXTRAORDINARY TRACE
f_N
f_T
16 msec
f_N
AMPLITUDE
f_T
ECHO
f_X
$2f_H$
$2f_T$
TIME

Figure 1

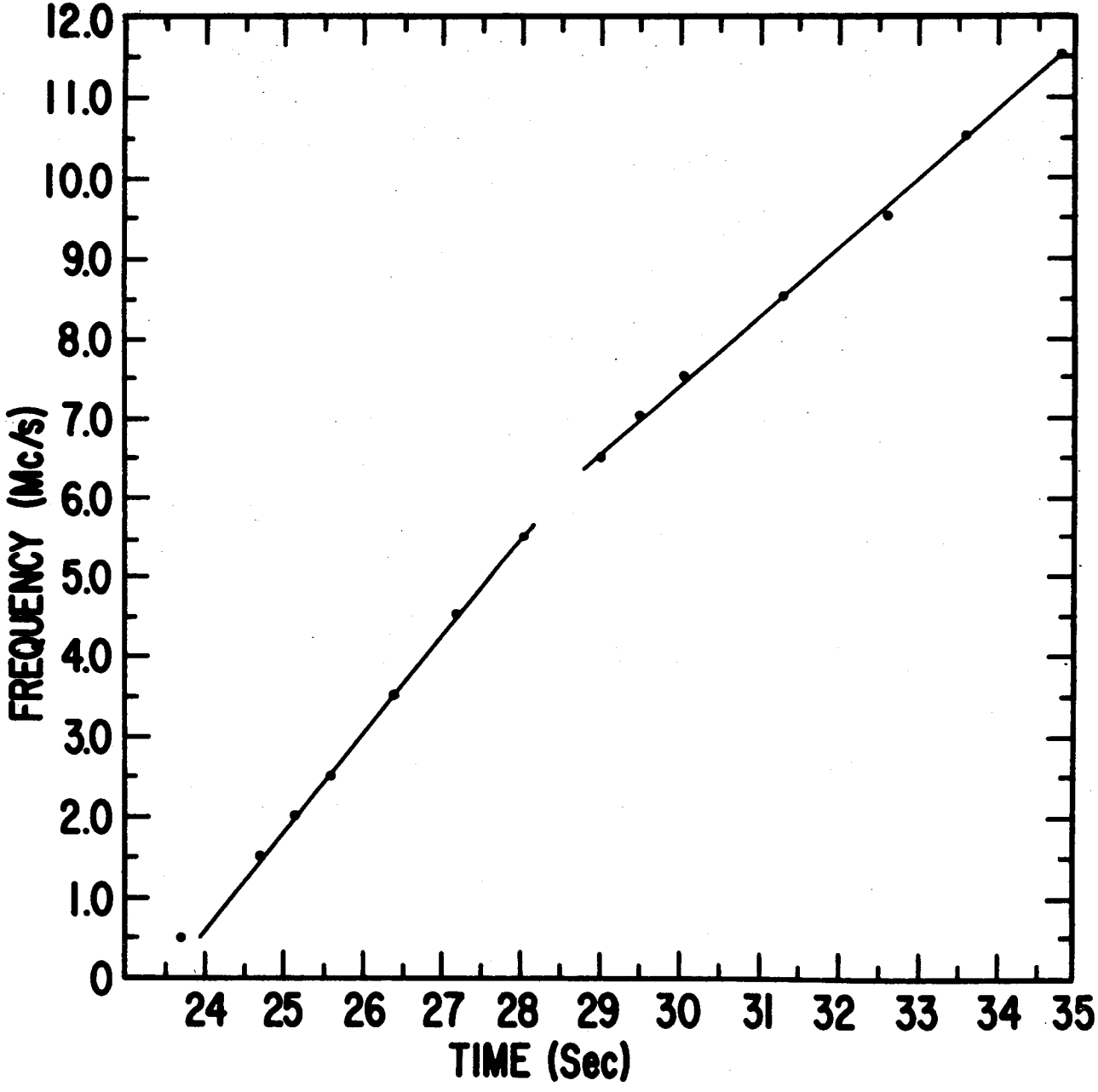
12.0
11.0
10.0
9.0
8.0
7.0
6.0
5.0
4.0
3.0
2.0
1.0
0
FREQUENCY (Mc/s)
24
25
26
27
28
29
30
31
32
33
34
35
TIME (Sec)

Figure 2

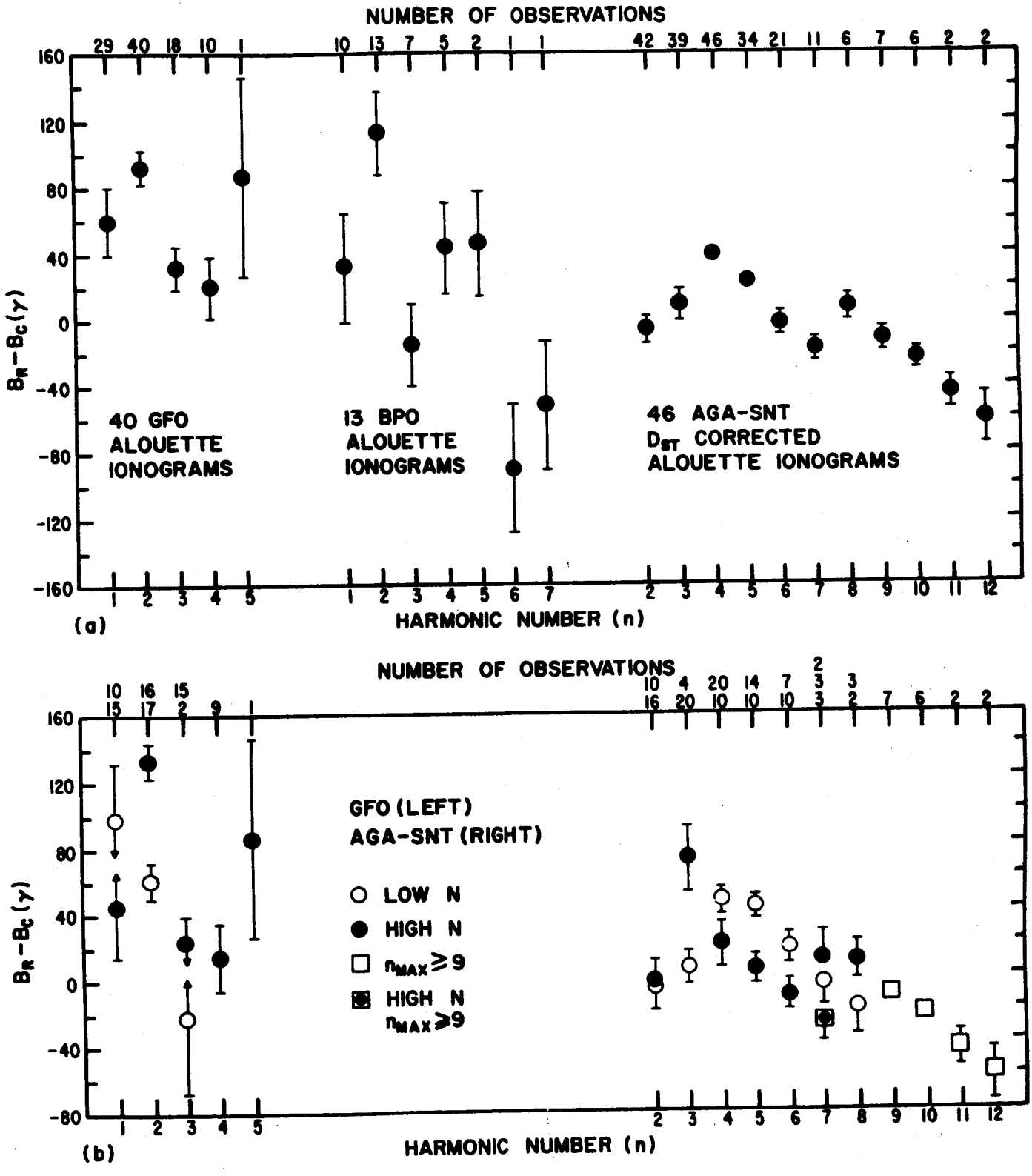
NUMBER OF OBSERVATIONS
29 40 18 10 1
10 13 7 5 2 1 1
42 39 46 34 21 11 6 7 6 2 2
160
120
80
40
0
-40
-80
-120
-160
$B_R - B_C(\gamma)$
40 GFO
ALOUETTE
IONOGRAMS
13 BPO
ALOUETTE
IONOGRAMS
46 AGA-SNT
D_{ST} CORRECTED
ALOUETTE IONOGRAMS
1 2 3 4 5
1 2 3 4 5 6 7
2 3 4 5 6 7 8 9 10 11 12
(a)
HARMONIC NUMBER (n)
NUMBER OF OBSERVATIONS
10 16 15
15 17 2 9 1
10 4 20 14 7 2 3 3
16 20 10 10 10 3 3 2 7 6 2 2
160
120
80
40
0
-40
-80
$B_R - B_C(\gamma)$
GFO (LEFT)
AGA-SNT (RIGHT)
LOW N
HIGH N
$n_{MAX} \geq 9$
HIGH N
$n_{MAX} \geq 9$
1 2 3 4 5
2 3 4 5 6 7 8 9 10 11 12
(b)
HARMONIC NUMBER (n)

Figure 3

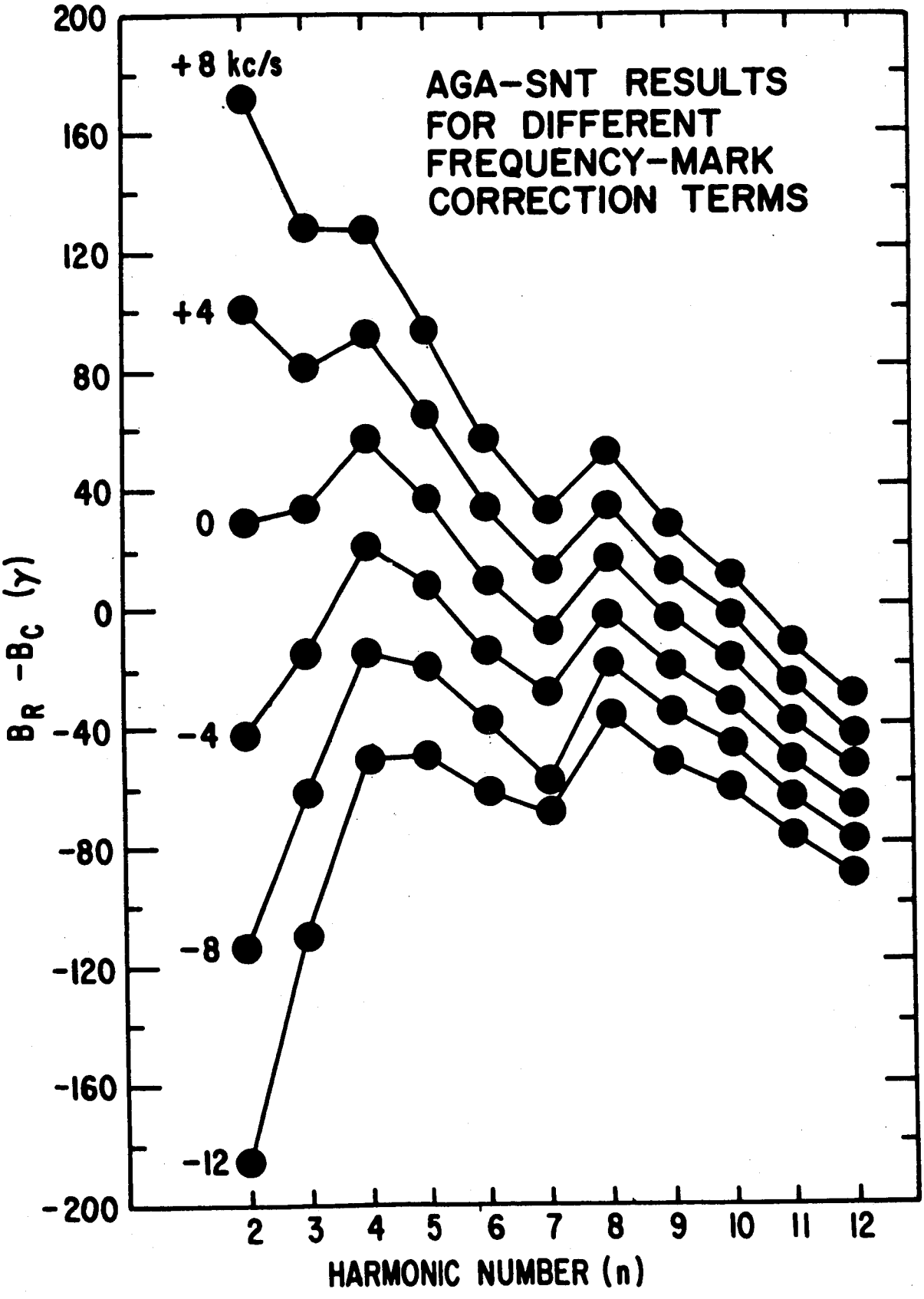
AGA-SNT RESULTS
FOR DIFFERENT
FREQUENCY-MARK
CORRECTION TERMS
+8 kc/s
+4
0
-4
-8
-12
200
160
120
80
40
0
-40
-80
-120
-160
-200
$B_R - B_C$ (γ)
2
3
4
5
6
7
8
9
10
11
12
HARMONIC NUMBER (n)

Figure 4

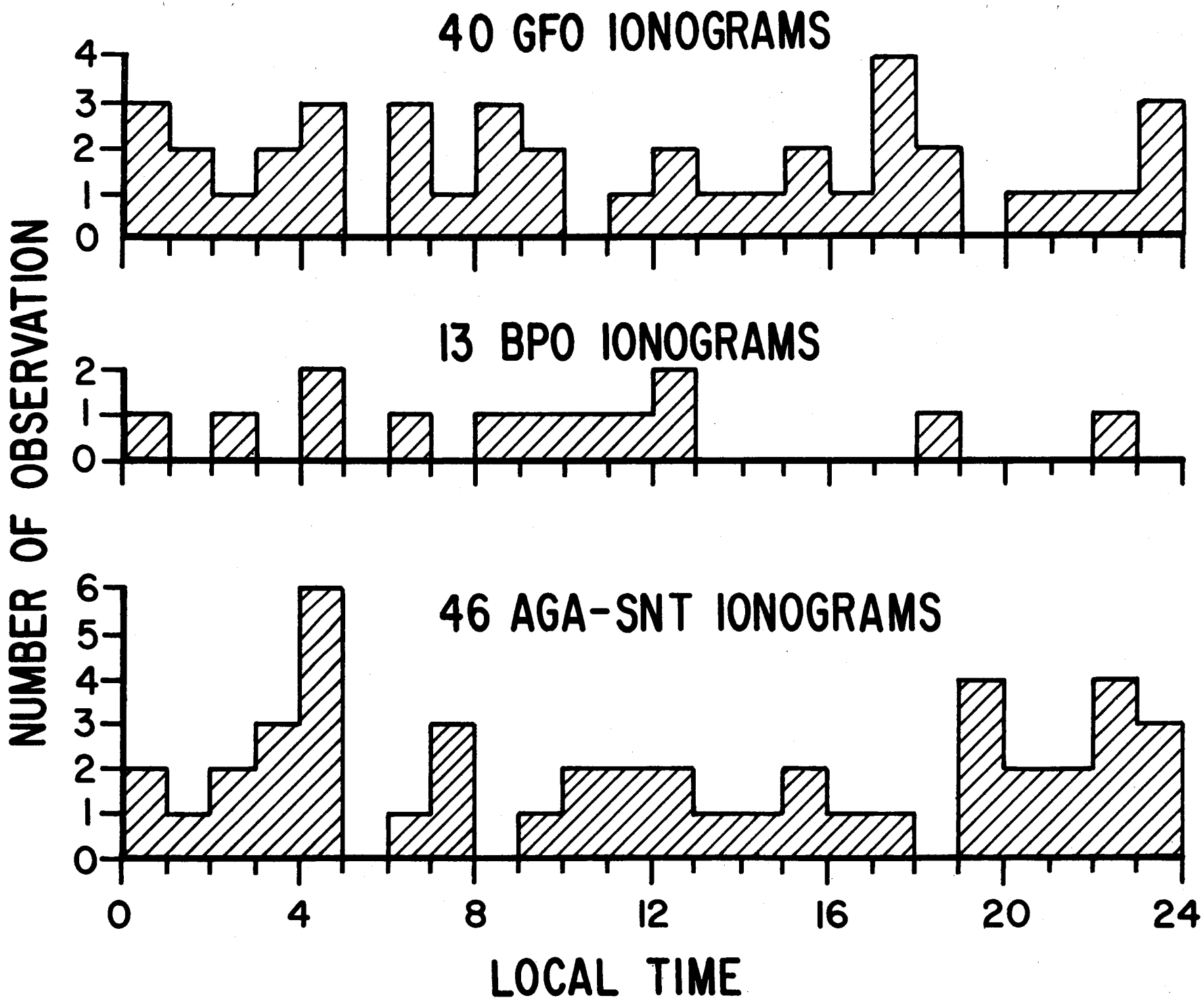
40 GFO IONOGRAMS
13 BPO IONOGRAMS
46 AGA-SNT IONOGRAMS
NUMBER OF OBSERVATION
LOCAL TIME
0
4
8
12
16
20
24

Figure 5

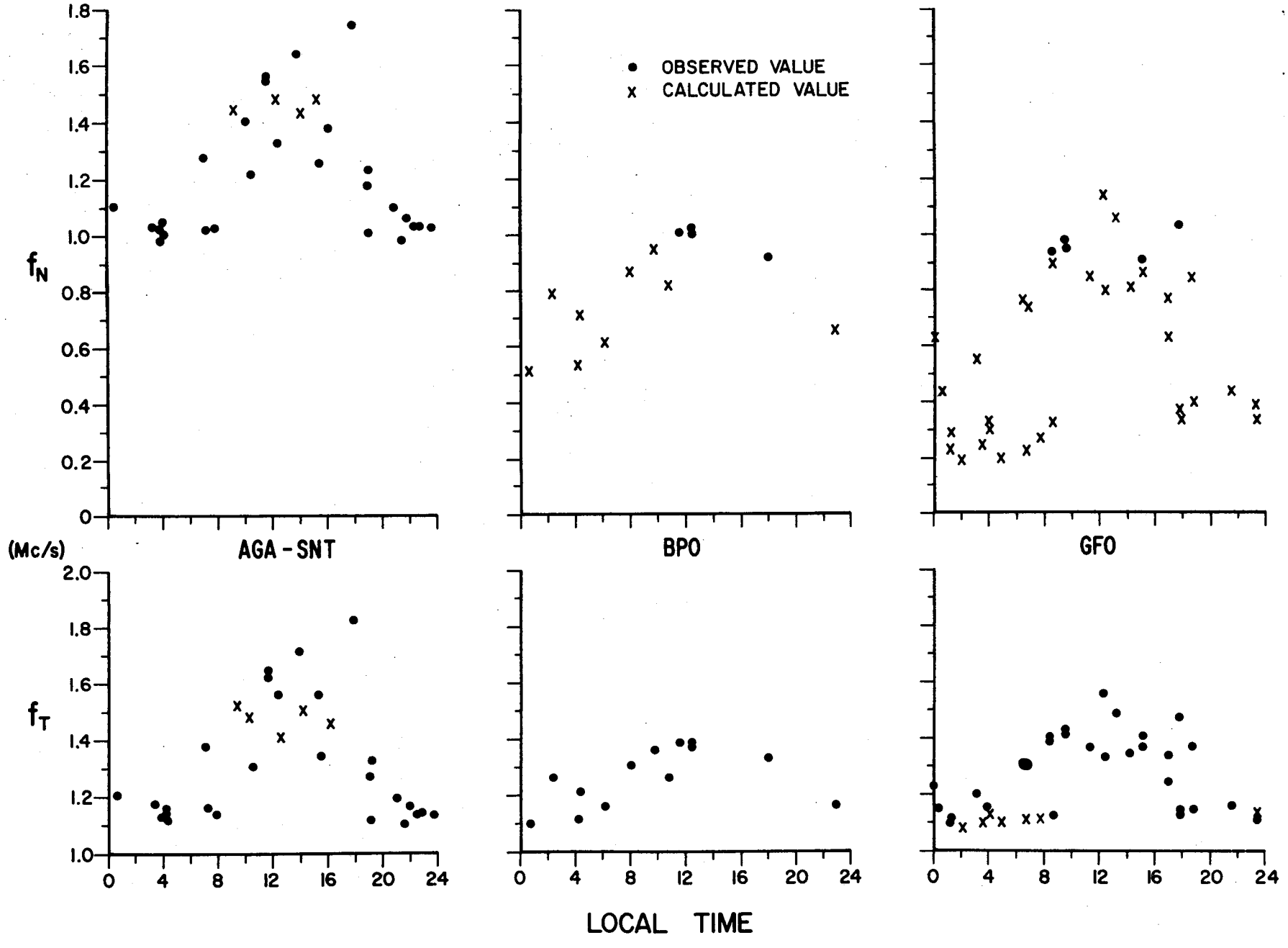
OBSERVED VALUE
CALCULATED VALUE
f_N
f_T
(Mc/s)
AGA - SNT
BPO
GFO
LOCAL TIME

Figure 6

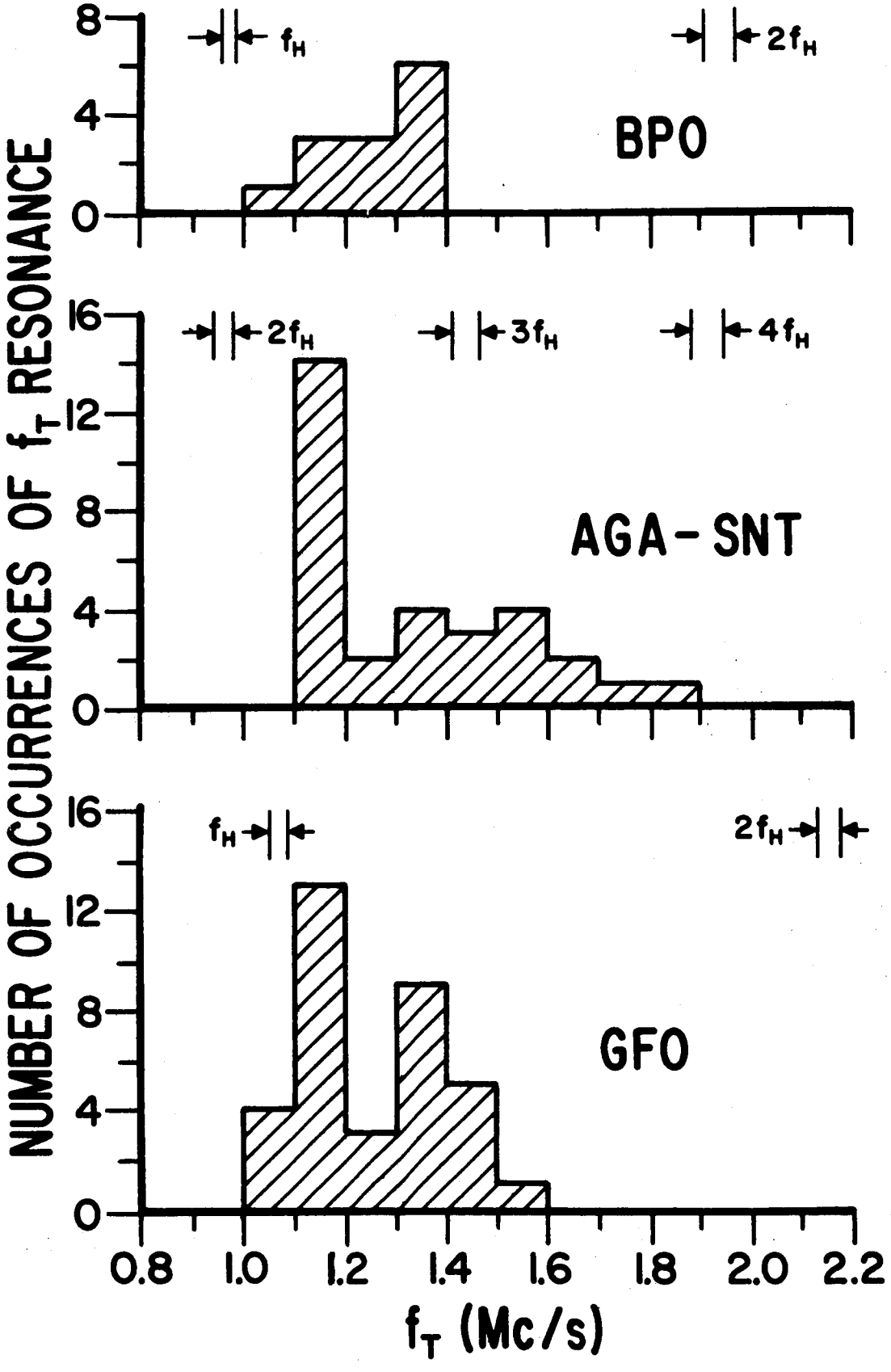
NUMBER OF OCCURRENCES OF f_T RESONANCE
BPO
AGA-SNT
GFO
f_H
$2f_H$
$3f_H$
$4f_H$
0
4
8
12
16
0.8
1.0
1.2
1.4
1.6
1.8
2.0
2.2
f_T (Mc/s)

Figure 7

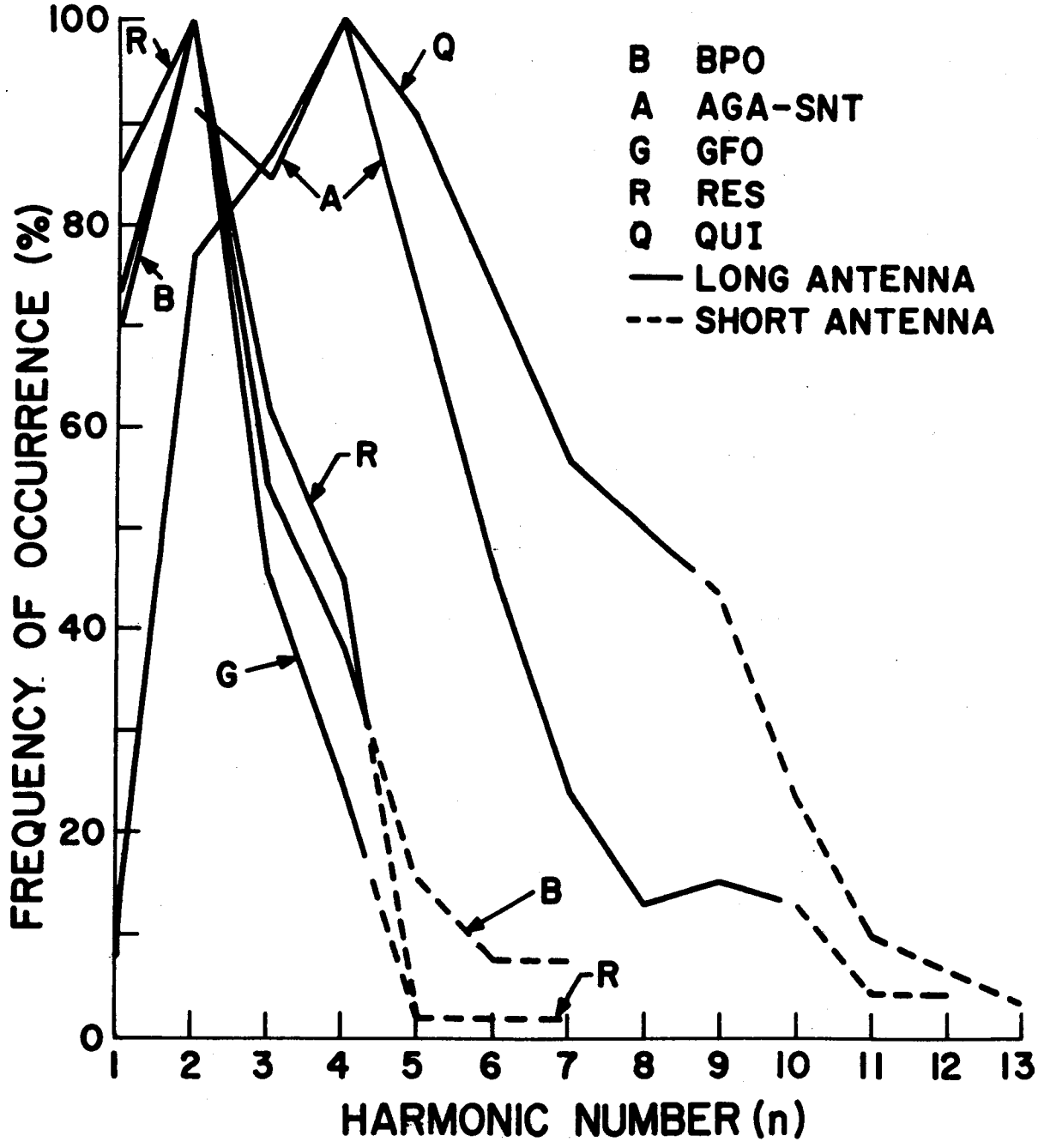
100
80
60
40
20
0
FREQUENCY OF OCCURRENCE (%)
1
2
3
4
5
6
7
8
9
10
11
12
13
HARMONIC NUMBER (n)
B BPO
A AGA-SNT
G GFO
R RES
Q QUI
LONG ANTENNA
SHORT ANTENNA
R
Q
A
B
R
G
B
R

Figure 8

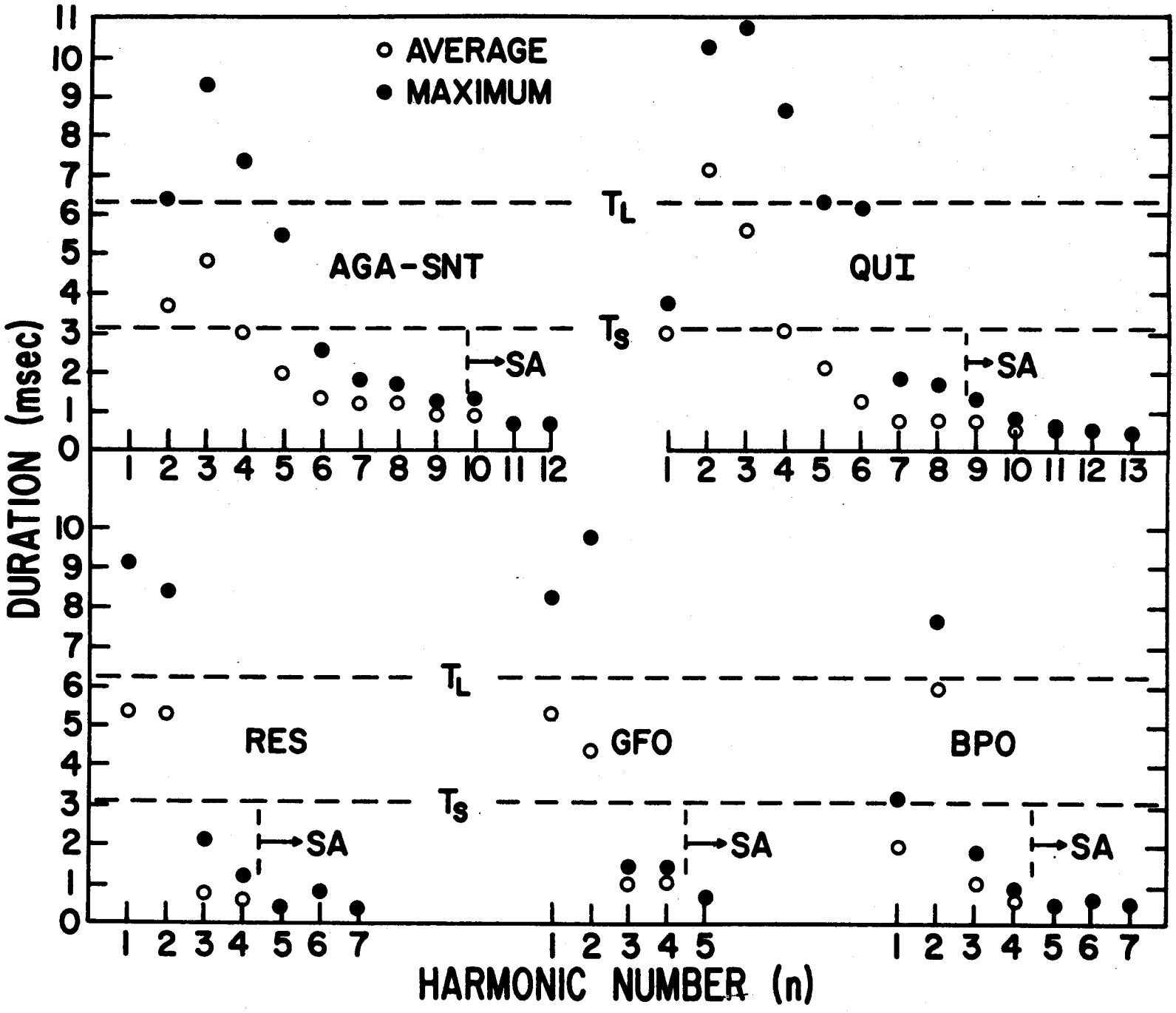
AVERAGE
MAXIMUM
AGA-SNT
QUI
RES
GFO
BPO
T_L
T_S
SA
DURATION (msec)
HARMONIC NUMBER (n)

Figure 9

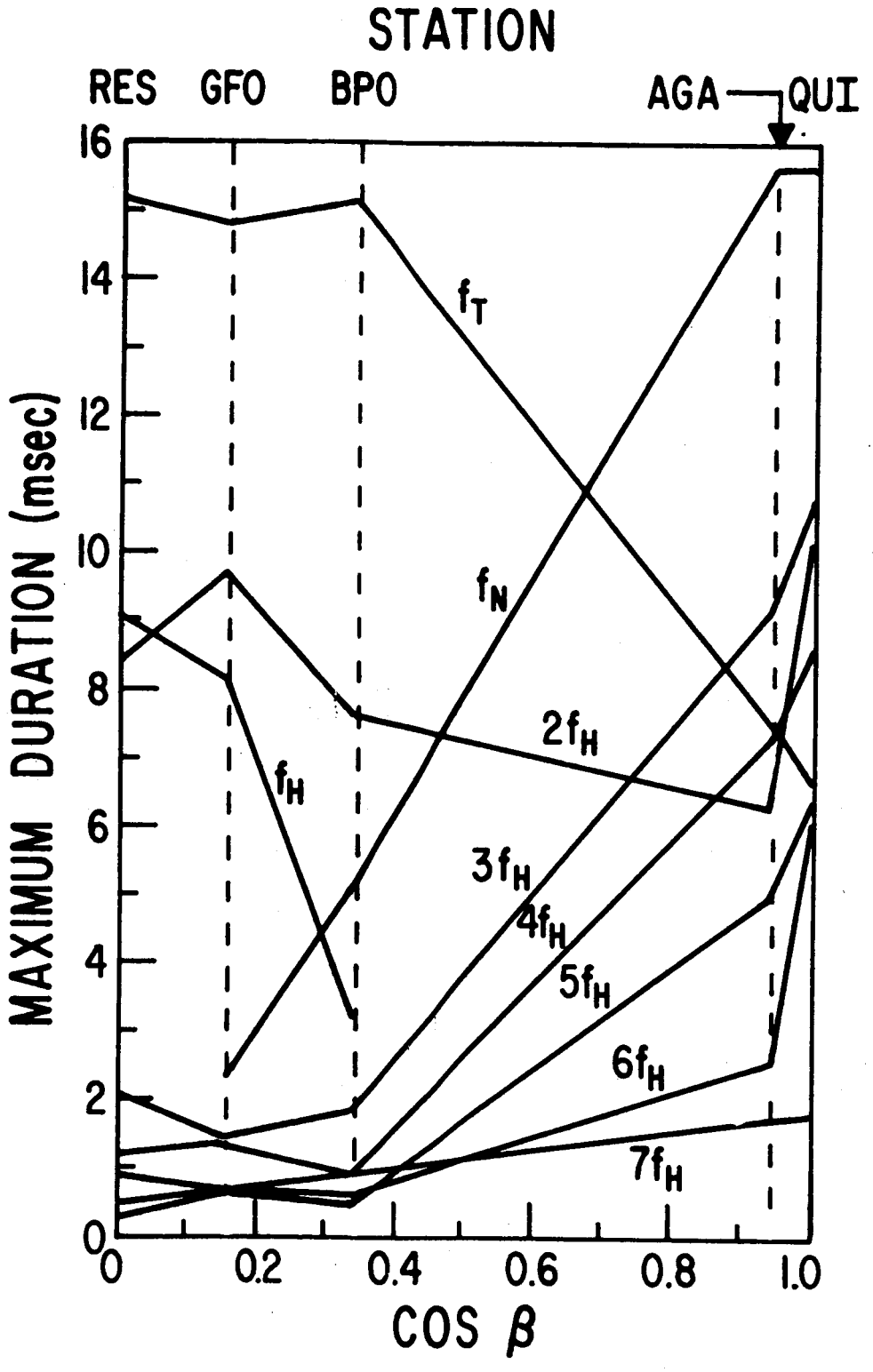
STATION
RES
GFO
BPO
AGA
QUI
MAXIMUM DURATION (msec)
16
14
12
10
8
6
4
2
0
0
0.2
0.4
0.6
0.8
1.0
COS β
f_T
f_N
f_H
$2f_H$
$3f_H$
$4f_H$
$5f_H$
$6f_H$
$7f_H$

Figure 10

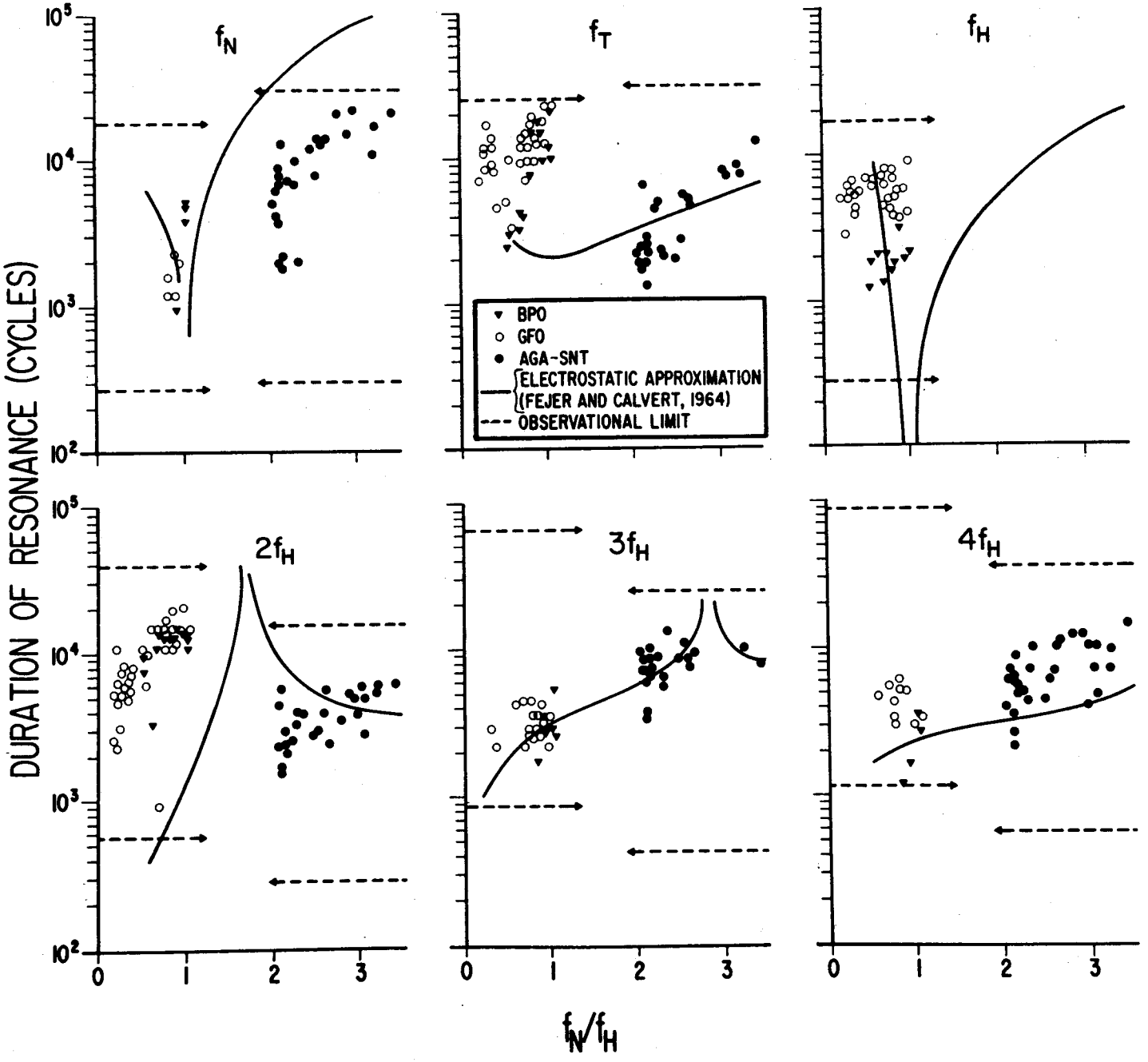
DURATION OF RESONANCE (CYCLES)
10^5
10^4
10^3
10^2
f_N
f_T
f_H
$2f_H$
$3f_H$
$4f_H$
BPO
GFO
AGA-SNT
ELECTROSTATIC APPROXIMATION
(FEJER AND CALVERT, 1964)
OBSERVATIONAL LIMIT
0
1
2
3
f_N/f_H

Figure 11

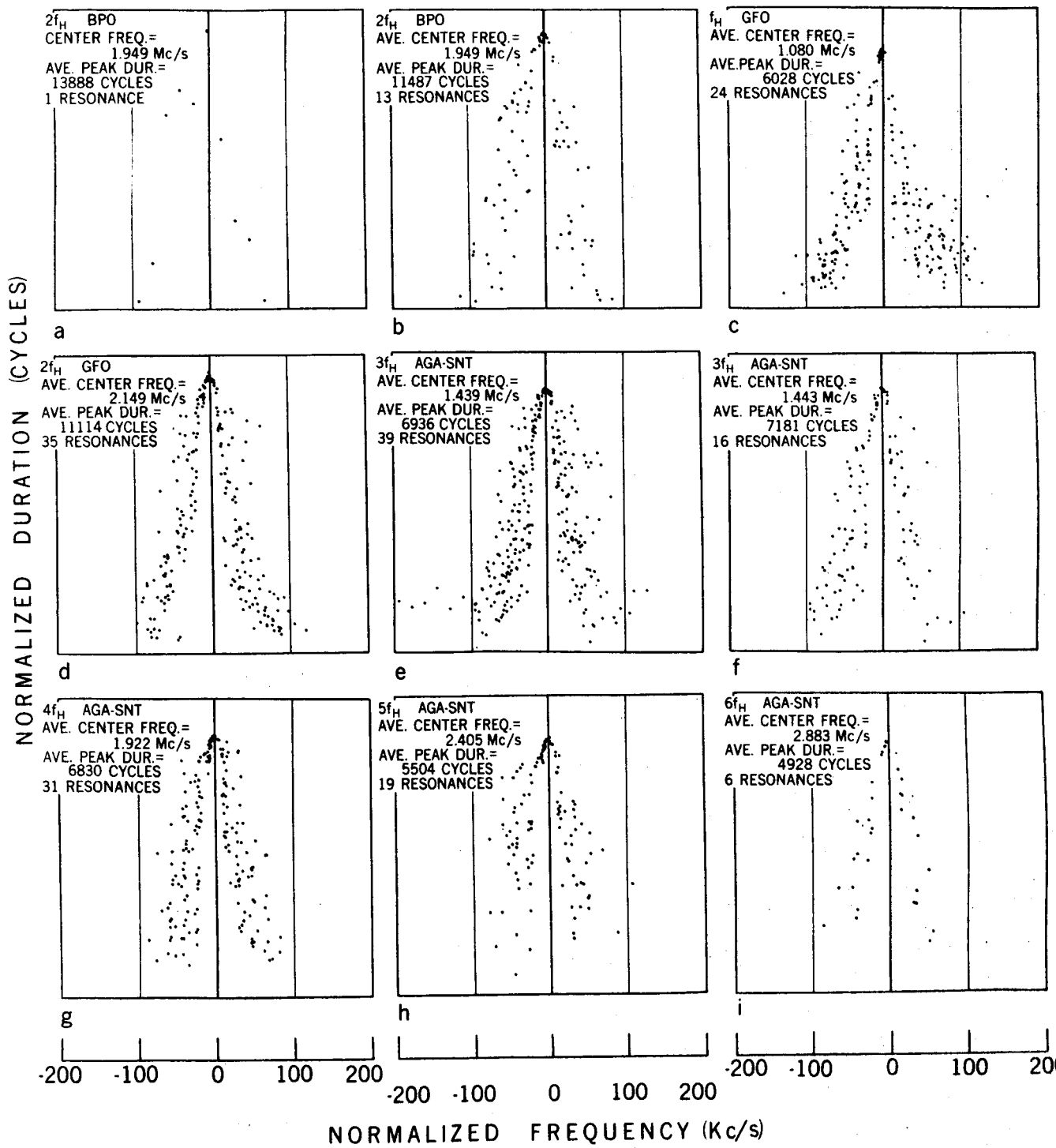
2f_H BPO
CENTER FREQ.=
1.949 Mc/s
AVE. PEAK DUR.=
13888 CYCLES
1 RESONANCE
a
2f_H BPO
AVE. CENTER FREQ.=
1.949 Mc/s
AVE. PEAK DUR.=
11487 CYCLES
13 RESONANCES
b
f_H GFO
AVE. CENTER FREQ.=
1.080 Mc/s
AVE.PEAK DUR.=
6028 CYCLES
24 RESONANCES
c
2f_H GFO
AVE. CENTER FREQ.=
2.149 Mc/s
AVE. PEAK DUR.=
11114 CYCLES
35 RESONANCES
d
3f_H AGA-SNT
AVE. CENTER FREQ.=
1.439 Mc/s
AVE. PEAK DUR.=
6936 CYCLES
39 RESONANCES
e
3f_H AGA-SNT
AVE. CENTER FREQ.=
1.443 Mc/s
AVE. PEAK DUR.=
7181 CYCLES
16 RESONANCES
f
4f_H AGA-SNT
AVE. CENTER FREQ.=
1.922 Mc/s
AVE. PEAK DUR.=
6830 CYCLES
31 RESONANCES
g
5f_H AGA-SNT
AVE. CENTER FREQ.=
2.405 Mc/s
AVE. PEAK DUR.=
5504 CYCLES
19 RESONANCES
h
6f_H AGA-SNT
AVE. CENTER FREQ.=
2.883 Mc/s
AVE. PEAK DUR.=
4928 CYCLES
6 RESONANCES
i
NORMALIZED DURATION (CYCLES)
-200 -100 0 100 200
-200 -100 0 100 200
-200 -100 0 100 200
NORMALIZED FREQUENCY (Kc/s)

Figure 12

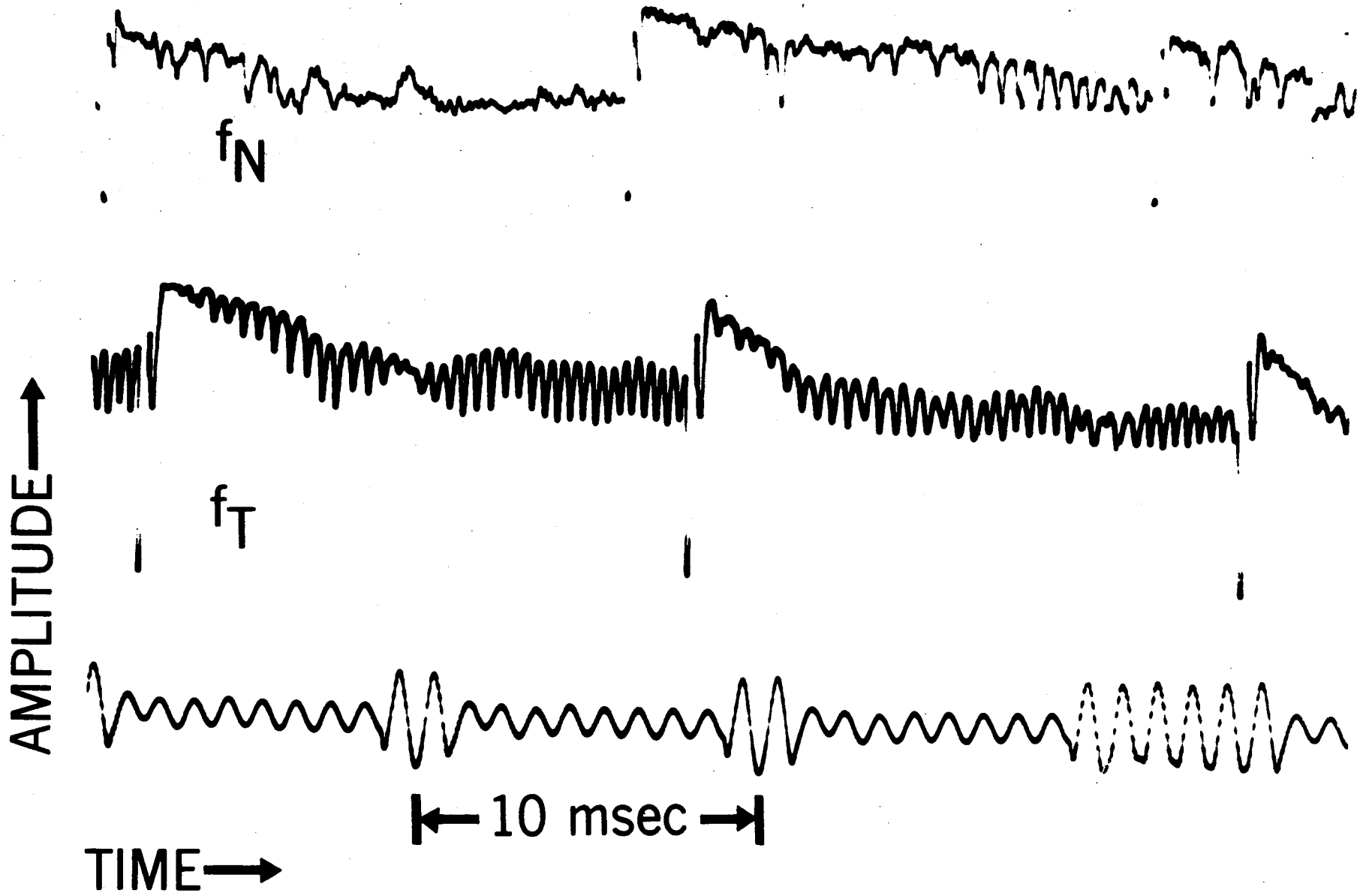

Figure 13

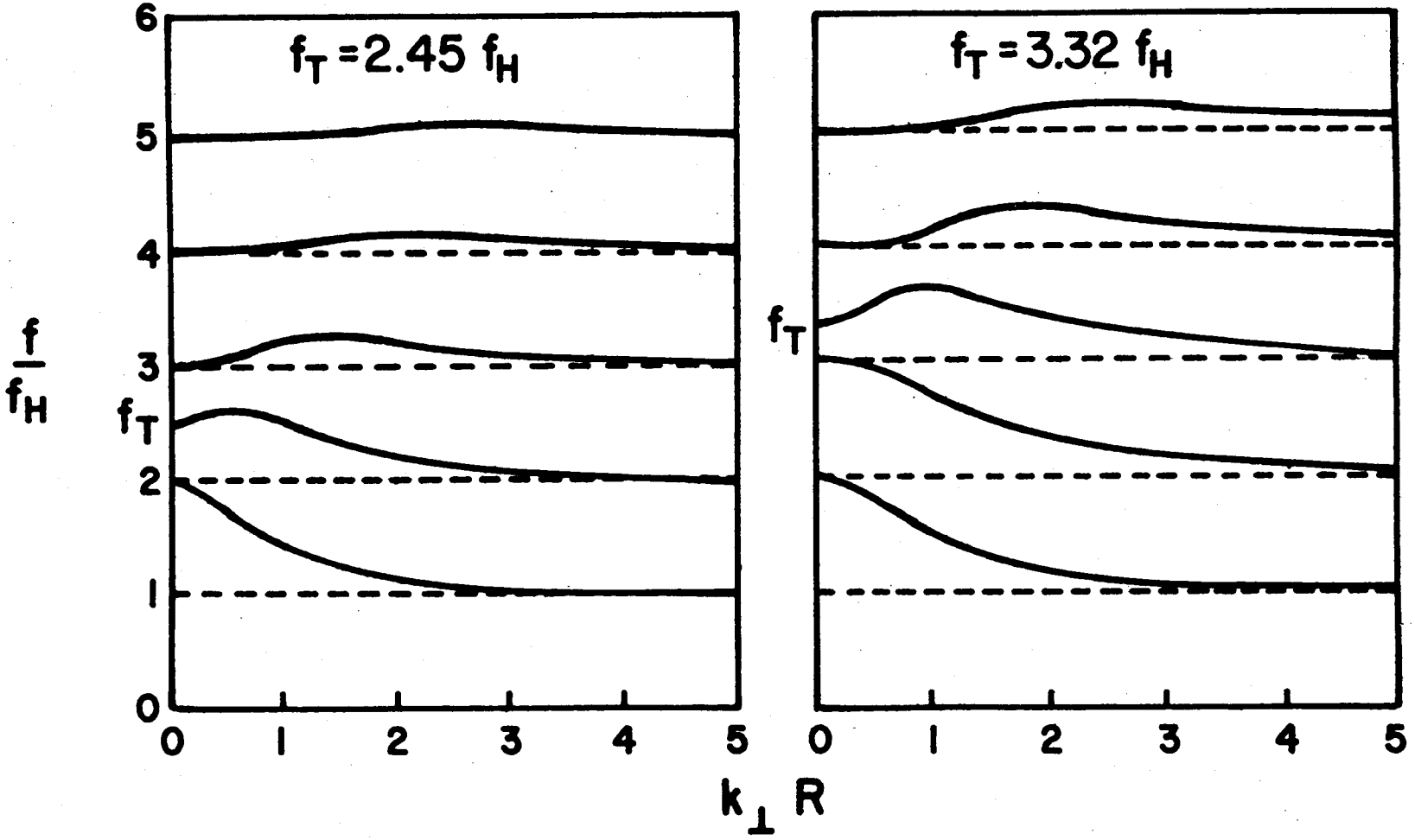

Figure 14